

The Free Precession and Libration of Mercury

S. J. Peale

Department of Physics

University of California

Santa Barbara, CA 93106

email: peale@io.physics.ucsb.edu

Abstract

An analysis based on the direct torque equations including tidal dissipation and a viscous core-mantle coupling is used to determine the damping time scales of $O(10^5)$ years for free precession of the spin about the Cassini state and free libration in longitude for Mercury. The core-mantle coupling dominates the damping over the tides by one to two orders of magnitude for the plausible parameters chosen. The short damping times compared with the age of the solar system means we must find recent or on-going excitation mechanisms if such free motions are found by the current radar experiments or the future measurement by the MESSENGER and BepiColombo spacecraft that will orbit Mercury. We also show that the average precession rate is increased by about 30% over that obtained from the traditional precession constant because of a spin-orbit resonance induced contribution by the C_{22} term in the expansion of the gravitational field. The C_{22} contribution also causes the path of the spin during the precession to be slightly elliptical with a variation in the precession rate that is a maximum when the obliquity is a minimum. An observable free precession will compromise the determination of obliquity of the Cassini state and hence of $C/M_M R^2$ for Mercury, but a detected free libration will not compromise the determination of the forced libration amplitude and thus the verification of a liquid core.

1. Introduction

A major goal of the MESSENGER (Solomon, et al. 2001) and BepiColombo (Anselmi & Scoon, 2001) missions to Mercury and ground-based Radar Speckle Displacement Interferometry (RSDI) observations (Holin, 1988, 1992, 2003; Margot *et al.* 2003) is the determination of the structure and state of Mercury’s interior. The probe of interior properties is based on the accurate determination of the four parameters, i , ϕ_0 , J_2 and C_{22} , where i is Mercury’s obliquity, ϕ_0 is the amplitude of the physical libration in longitude, and J_2 and C_{22} are the second degree harmonic coefficients in the expansion of Mercury’s gravitational field. These parameters are sufficient for determining the factors in the equation (Peale, 1976a; 1981; 1988; Peale *et al.* 2002)

$$\left(\frac{C_m}{B-A}\right) \left(\frac{B-A}{M_M R^2}\right) \left(\frac{M_M R^2}{C}\right) = \frac{C_m}{C} \leq 1, \quad (1)$$

where M_M and R are the mass and radius of Mercury, $A < B < C$ are the principal moments of inertia, and C_m is the polar moment of inertia of the mantle alone.

The first factor follows from the amplitude of the physical libration

$$\phi_0 = \frac{3}{2} \left(\frac{B-A}{C_m}\right) \left(1 - 11e^2 + \frac{959}{48}e^4 + \dots\right), \quad (2)$$

where e is the orbital eccentricity, and C_m occurs in the denominator because a liquid core is not expected to follow the 88 day physical libration of the mantle. The second factor follows from

$$\frac{B-A}{M_M R^2} = 4C_{22}, \quad (3)$$

and the third from (Peale, 1969)

$$\frac{C}{M_M R^2} = \frac{\left[J_2 / (1 - e^2)^{3/2} + 2C_{22} \left(\frac{7}{2}e - \frac{123}{16}e^3 \right) \right] n}{(\sin I) / i_c - \cos I} \frac{1}{\mu}, \quad (4)$$

where i_c is the obliquity of Cassini state 1, (*E.g.*, Colombo, 1966; Peale, 1969), which Mercury is expected to occupy ($i = i_c$), I is the inclination of the orbit plane to the Laplace plane on which Mercury’s orbit precesses at the constant rate $-\mu$, and n is the orbital mean motion, and the equation assumes $i_c \ll 1$. In a Cassini state the spin axis is coplanar with the normal to the Laplace plane and the orbit normal as both the spin and the orbit normal precess around the Laplace plane normal with an approximately 280,000 year period. Fig. 1 shows the configuration for Cassini state 1, where the ascending node of the equator plane on the orbit plane remains coincident with the ascending node of the orbit plane on the Laplace plane. In Fig. 1, the Z axis is normal to the orbit plane, the Y axis is in the orbit plane, and the X axis comes out of the paper. Eq. (4) shows the dependence of $C/M_M R^2$ on J_2 , C_{22}

and i_c , and together, the last three equations show the necessity of knowing i_c , ϕ_0 , J_2 and C_{22} to determine C_m/C .

[Figure 1]

Conditions for the success of the experiment are

- 1) The liquid core must not follow the mantle during the 88 day forced libration in longitude.
- 2) The core must follow the mantle during the 280,000 year orbit precession, where the spin axis is locked to this precession if it occupies the Cassini state.
- 3) $B - A$ must be due to the mantle alone.
- 4) Adiabatic invariance must keep the spin close to the Cassini state during the slow variation of the orbital elements.

The first two conditions are satisfied for viscous core-mantle coupling, topographical coupling due to core-mantle boundary (CMB) irregularities, magnetic core-mantle coupling, and gravitational coupling between an axially asymmetric solid inner core and the mantle (Peale, et al. 2002). The third condition requires that there not be long wavelength irregularities in the CMB such that dense core material contributes to $B - A$. Such irregularities could be induced by mantle convection (D. Stevenson, private communication, 2003), but a major contribution to $B - A$ would occur only if the convective cells have circumferential scales comparable to the planet radius R . Otherwise, the plus and minus contributions due to short wavelength topography would tend to average to a zero total contribution to $B - A$. As the iron core must be near $0.75R$ in radius (Siegfried and Solomon, 1974), the horizontal scale of any convective cells is unlikely to greatly exceed the $0.25R$ thickness of the mantle. It has also been argued that Mercury’s mantle convection ceased early in Mercury’s history (Reese and Peterson, 2002), and the CMB should thereby be nearly axially symmetric with little or no contribution to $B - A$ from the core.

It is implicitly assumed in the above that all free motions associated with Mercury’s spin are damped to near zero amplitude, and that the spin remains close to the current location of Cassini state 1 in spite of slow variation of the orbital parameters that define the state. The free motions include a free libration in longitude, a free precession of the spin about Cassini state 1, and a free wobble. The free libration in longitude results when the axis of minimum moment of inertia does not point toward the Sun when Mercury is at perihelion. The gravitational torque on the permanent asymmetry of the planet, averaged around the orbit, tends to restore the alignment of the axis of minimum moment of inertia with the Sun at perihelion because of the 3:2 spin-orbit resonance, so viewed at perihelion, the long axis will tend to librate about the direction toward the Sun with a period of about 10 years. The free precession of the spin axis is like the 26,000 year precession of the Earth’s spin axis about the ecliptic, except the precession is about the Cassini state instead of the orbit normal, where the deviation of the Cassini state from the orbit normal is less than 2 arcmin. The period of this precession is $O(1000 \text{ years})$. Free wobble or non principal axis rotation occurs when the spin axis does not coincide with the axis of maximum moment of inertia. The

spin axis then precesses around the axis of maximum moment of inertia in the body frame of reference with a period $O(500 \text{ years})$. The wobble is analogous to the Chandler wobble of the Earth. The angular momentum is conserved during free wobble, and the spin axis makes only small excursions relative to inertial space. The spin angular momentum is not conserved during the free libration and free precession as the planet responds to the external gravitational torque due to the Sun. In the former the spin axis direction is maintained as the magnitude of the spin varies periodically, whereas in the latter the spin describes a cone about the Cassini state, which is almost a cone relative to inertial space.

The term “free” characterizes these motions as having arbitrary phases and amplitudes, which amplitudes, if significantly different from zero, could complicate the interpretation of the spacecraft and radar data constraining the properties of the interior. For example, a finite amplitude free precession would displace Mercury’s spin vector from the Cassini state, and its arbitrary phase and amplitude would thereby increase the uncertainty in the obliquity of the state used in determining $C/M_M R^2$ in Eq. (4). Tidal friction has been shown to carry the spin to Cassini state 1 from almost any initial configuration on a time scale that is short compared to the age of the solar system (Peale, 1974; Ward, 1975). Free libration in longitude (9.2 year period, for $(B - A)/C_m = 3.5 \times 10^{-4}$) is similarly damped, but such a free libration does not confuse the experiment, as the 88 day forced libration is superposed on the free libration (Peale, *et al.* 2002), and its amplitude is readily discernible. Any free wobble will also damp due to dissipation by internal friction as the equator plane changes relative to the body principal axis system in addition to tidal friction and core-mantle dissipation. For the Moon, tidal dissipation is about 4 times more effective than the dissipation caused by the changing orientation of the equator (Peale, 1976b). Finally it was asserted (Peale, 1974) that the spin would remain close to the instantaneous position of the Cassini state if it were ever close because of the adiabatic invariance of an action integral that is equivalent to the solid angle swept out by the spin vector as it precesses around the Cassini state.

If, on the other hand, free motions of measurable amplitude are found, excitation mechanisms must be sought given the damping. Relatively small amplitudes of free motions can be detected by orbiting spacecraft (Zuber and Smith, 2000) and radar (Holin, 2003; Margot *et al.* 2003). The damping time scales constrain the types of excitation mechanisms that are likely to be responsible. For example, short time scales make excitation by the impact of large objects less likely (See Section 4). The existence of a liquid core introduces damping by core-mantle interaction that shortens the time scales for the damping of free motions deduced for tidal dissipation. This paper is the first of three where we consider the free motions and quantify the adiabatic invariance of the spin axis separation from the Cassini state. Here we derive and compare damping time scales for the two processes of tidal friction and core-mantle dissipation with viscous coupling for free libration and free precession. Quantifying the adiabatic invariance and determining the damping of a free wobble require different approaches, and these will be considered in the following papers. The damping of the free rotational motions of the Moon have been determined earlier using a Hamiltonian

formulation with dissipation accounted for by introducing phase lags in the periodic terms describing the response of the Moon to various forcing potentials (Peale, 1976b). This analysis is general albeit somewhat complicated. For the libration and precession considered here we use a much simpler approach by fixing the orbit and writing the equations of motion directly in terms of the external and internal torques on the mantle and core. However, this simplified approach will not work well for the wobble, so the general Hamiltonian analysis will be used in a following paper to treat the wobble damping, although the torque equations will be applied there for the core-mantle coupling. In Sections 2 and 3, we show that the damping times for the free precession and the free libration in longitude are both near 10^5 years with the core-mantle interaction being between one and two orders of magnitude more effective than tidal friction. In Section 4 we show that the time between impacts capable of generating observable amplitudes of free libration or precession exceeds 10^9 years, making such excitation exceedingly unlikely. Summary and conclusions follow in Section 5. We begin with the free precession, as the equations describing the damping of the libration in longitude are scalar versions of those describing the damping of the precession.

2. Damping of free precession

Generally, the spin axis precesses about Cassini state 1 which is offset approximately 1.7 arcmin from the orbit normal. However, for the purposes of calculating the damping, we assume the orbit is fixed, so that the precession will be about the orbit normal. (The Cassini state for a fixed orbit can be thought to coincide with the orbit normal, since the state approaches the orbit normal as the orbital precession rate is decreased, or it can be thought not to exist at all.) Accordingly, we adopt an XYZ inertial system centered on Mercury with the XY plane coincident with the orbit plane, the X axis pointing from Mercury to the perihelion of the Sun’s relative orbit, and with unit vector $\mathbf{e}_o = \mathbf{e}_z$ being the orbit normal. During the precession about the orbit normal, the damping of the precession angle about the orbit normal will be essentially the same as the damping of the precession about the Cassini state without involving the complications induced by the orbit precession. (See Peale, (1976b) for a complete analysis applied to the Moon.)

We assume that the core mantle interaction is simply proportional to the difference in the vector spin angular velocities of the mantle and core as the simplest possible coupling. This coupling is consistent with a viscous coupling between two rigid spheres. Mercury is rotating slowly enough such that pressure coupling of the core and mantle from the elliptical shape of the core-mantle boundary is not important, which leaves viscous coupling the most probable. We also assume principal axis rotation. The equations describing the motions of the core and mantle are then

$$C_m \ddot{\vec{\psi}}_m = \vec{N} + \vec{T} - k(\dot{\vec{\psi}}_m - \dot{\vec{\psi}}_c)$$

$$C_c \ddot{\vec{\psi}}_c = k(\dot{\vec{\psi}}_m - \dot{\vec{\psi}}_c), \quad (5)$$

where $\dot{\vec{\psi}}_{m,c}$ are the angular velocities of the mantle and core respectively, $C_{m,c}$ are the moments of inertia about the spin axis of the mantle and core, k is the coupling constant for the core-mantle torque, \vec{N} is the torque on Mercury's permanent figure due to the Sun, and \vec{T} is the tidal torque. We first describe the free precession of Mercury, which is affected by the spin-orbit resonance $\langle \dot{\psi}_m \rangle = 1.5n$, where $\langle \dot{\psi}_m \rangle$ is the average value of the magnitude of $\dot{\vec{\psi}}_m$, and n is the mean motion.

2.1. Free Precession

We start with the first of Eqs. (5), with $\vec{T} = k = 0$ and keep only the second order terms in the expansion of Mercury's gravitational potential Φ . Then the torque on Mercury is the negative of the torque on the Sun, so

$$\begin{aligned} \vec{r} \times \nabla \Phi = \vec{N} &= -\frac{GM_M M_\odot R^2}{r^3} \left[6C_{22} \sin \theta \sin 2\phi \mathbf{e}_\theta \right. \\ &+ \left. (3J_2 \sin \theta \cos \theta + 6C_{22} \sin \theta \cos \theta \cos 2\phi) \mathbf{e}_\phi \right], \end{aligned} \quad (6)$$

where G is the gravitational constant, M_M and M_\odot are the masses of Mercury and the Sun respectively, R is Mercury's radius, J_2 and C_{22} are second order harmonic coefficients in the expansion of Mercury's gravitational field, $r\theta\phi$ are the spherical polar coordinates of the Sun relative to the principal xyz axis system with \mathbf{e}_θ and \mathbf{e}_ϕ being unit vectors in the θ and ϕ directions. The z axis is the axis of maximum moment of inertia coincident with the spin axis, and x and y are axes of minimum and intermediate moments of inertia in the equator plane. We define $\hat{\mathbf{m}} = \mathbf{e}_z$ as a unit vector along the spin axis of the mantle. The xyz axes are oriented with respect to the XYZ axes through Euler angles Ω, i, ψ_m as shown in Fig. 2, where Ω is the longitude of the ascending node of the equator on the orbit plane, i is the obliquity, and ψ_m is the angle between the node and the x axis in the equator plane, with the subscript m again referring to the mantle.

[Figure 2]

The expression for \vec{N} in spherical coordinates relative to the body axes (Eq. (6)) is written in terms of the xyz components, and these are transformed to the XYZ components through the usual series of three rotations through the Euler angles. With the unit vector toward the Sun, $\hat{\mathbf{r}} = \cos f \mathbf{e}_x + \sin f \mathbf{e}_y = \sin \theta \cos \phi \mathbf{e}_x + \sin \theta \sin \phi \mathbf{e}_y + \cos \theta \mathbf{e}_z$, where $\mathbf{e}_{X,Y,Z}$ and $\mathbf{e}_{x,y,z}$ are unit vectors along the respective axes, scalar products $\hat{\mathbf{r}} \cdot \mathbf{e}_x, \mathbf{e}_y, \mathbf{e}_z$ yield the expressions for the products of circular functions of the spherical coordinates in \vec{N} in terms of the Euler angles and the true anomaly f when $\mathbf{e}_{x,y,z}$ are expressed in the XYZ system. These results and the transformation yield \vec{N} in the XYZ system in terms of the Euler

angles and the true anomaly.

$$\begin{aligned}
\vec{N} = & -\frac{GM_\odot M_M R^2}{r^3} \left\{ 3J_2 \sin i \cos i \sin(f - \Omega) [\sin f \mathbf{e}_x - \cos f \mathbf{e}_y] \right. \\
& - 1.5J_2 \sin i \sin 2(f - \Omega) \mathbf{e}_z \\
& + 6C_{22} \sin i [\cos i \cos 2\psi \sin(f - \Omega) - \cos(f - \Omega) \sin 2\psi] (-\sin f \mathbf{e}_x + \cos f \mathbf{e}_y) \\
& \left. + 6C_{22} \left[-\frac{3 + \cos 2i}{4} \sin 2(f - \Omega) \cos 2\psi + \cos i \cos 2(f - \Omega) \sin 2\psi \right] \mathbf{e}_z \right\} \quad (7)
\end{aligned}$$

To eliminate high frequency terms due to the orbital motions, we average Eq. (7) over an orbit period keeping everything constant except f and ψ_m . With $\dot{\psi}_m = 1.5n$ ($n =$ mean motion), we can write $\psi_m = \psi_{m0} + 1.5M$, where M is the mean anomaly and ψ_{m0} is constant over the orbit period. With this substitution for ψ_m , we expand the circular functions in Eq. (7) to display products of circular functions of f and M with a^3/r^3 . The terms yielding non zero averages over the orbit period are then

$$\begin{aligned}
\left\langle \frac{a^3}{r^3} \right\rangle &= \frac{1}{2\pi} \int_0^{2\pi} \frac{a^3}{r^3} \frac{dM}{df} df = \frac{1}{(1 - e^2)^{3/2}} \\
\left\langle \frac{a^3}{r^3} \cos 3M \right\rangle &= \frac{53e^3}{16} + \dots \\
\left\langle \frac{a^3}{r^3} \cos 2f \cos 3M \right\rangle &= \frac{1}{2} \left(\frac{7}{2}e - \frac{123}{16}e^3 + \dots \right) \\
\left\langle \frac{a^3}{r^3} \sin 2f \sin 3M \right\rangle &= \frac{1}{2} \left(\frac{7}{2}e - \frac{123}{16}e^3 + \dots \right), \quad (8)
\end{aligned}$$

where $r = a(1 - e^2)/(1 + e \cos f)$ and $dM/df = r^2/(a^2\sqrt{1 - e^2})$ have been used. Some of these averages are easily done directly, whereas others are easily evaluated with the help of Cayley's (1859) tabulated expansions.

When $M = 0$, the x axis is nearly aligned with the X axis as a condition of the spin-orbit resonance. This will be true for small i if $\psi_{m0} = -\Omega$. With this substitution, the averaged torque on the permanent asymmetric figure of Mercury is

$$\begin{aligned}
\langle \vec{N} \rangle = & -n^2 M_M R^2 \left\{ \left[\frac{3J_2 \sin i \cos i}{2(1 - e^2)^{3/2}} + \frac{3C_{22} \sin i(1 + \cos i)}{2} \left(\frac{7}{2}e - \frac{123}{16}e^3 \right) \right] \times \right. \\
& (\cos \Omega \mathbf{e}_x + \sin \Omega \mathbf{e}_y) \\
& + \frac{3C_{22} \sin i(1 + \cos i)}{2} \frac{53}{16} e^3 (-\cos \Omega \mathbf{e}_x + \sin \Omega \mathbf{e}_y) \\
& \left. + \frac{3C_{22} \sin i(1 - \cos i)}{2} \frac{53}{16} e^3 (\cos 3\Omega \mathbf{e}_x + \sin 3\Omega \mathbf{e}_y) \right\}, \quad (9)
\end{aligned}$$

where the Z components average to zero—the Z component with coefficient J_2 because $\langle (a^3/r^3) \cos 2f \rangle = \langle (a^3/r^3) \sin 2f \rangle = 0$, and the Z component with coefficient C_{22} because $\sin(2\psi_{m0} + 2\Omega)$ vanishes with $\psi_{m0} = -\Omega$. The first bracketed factor shows how the traditional precession constant, involving only J_2 , has been modified by the spin-orbit resonance

with the addition of the C_{22} term, which decreases the precession period by nearly 30% from that due to the J_2 term alone. (For the Earth, only J_2 is important in determining the rate of precession, since terms involving C_{22} for the noncommensurate, rapid spin average to zero, and in addition, $C_{22} \ll J_2$.)

Before writing $\langle \vec{N} \rangle$ in a form suitable for solving the equations for the spin vector motion, it is instructive to write Eq. (9) in a different way. The following identities are needed.

$$\begin{aligned} \cos \Omega \mathbf{e}_X - \sin \Omega \mathbf{e}_Y &= \cos 2\Omega (\cos \Omega \mathbf{e}_X + \sin \Omega \mathbf{e}_Y) \\ &\quad + \sin 2\Omega (\sin \Omega \mathbf{e}_X - \cos \Omega \mathbf{e}_Y) \\ \sin i (\cos \Omega \mathbf{e}_X + \sin \Omega \mathbf{e}_Y) &= -\hat{\mathbf{m}} \times \mathbf{e}_Z \\ \sin i (\sin \Omega \mathbf{e}_X - \cos \Omega \mathbf{e}_Y) &= -(\hat{\mathbf{m}} \times \mathbf{e}_Z) \times \mathbf{e}_Z \end{aligned} \tag{10}$$

If we rearrange terms and employ some trigonometric identities along with Eqs. (10) in Eq. (9), we can write

$$\begin{aligned} \frac{\langle \vec{N} \rangle}{C_m \dot{\psi}_m} &= [K_1 \cos i + K_3 (1 - \cos i)] (\hat{\mathbf{m}} \times \mathbf{e}_Z) \\ &\quad - K_2 \cos i \cos 2\Omega (\hat{\mathbf{m}} \times \mathbf{e}_Z) \\ &\quad - K_2 \sin 2\Omega (\hat{\mathbf{m}} \times \mathbf{e}_Z) \times \mathbf{e}_Z. \end{aligned} \tag{11}$$

The constants $K_{1,2,3}$ are defined by

$$\begin{aligned} K_1 &= \frac{n^2 M_M R^2}{C_m \dot{\psi}_m} \left[\frac{3J_2}{2(1-e^2)^{3/2}} + 3C_{22} \left(\frac{7}{2}e - \frac{123}{16}e^3 \right) \right], \\ K_2 &= \frac{3n^2 M_M R^2}{C_m \dot{\psi}_m} C_{22} \frac{53}{16} e^3, \\ K_3 &= \frac{3n^2 M_M R^2}{2C_m \dot{\psi}_m} C_{22} \left(\frac{7}{2}e - \frac{123}{16}e^3 \right) \end{aligned} \tag{12}$$

The $\hat{\mathbf{m}} \times \mathbf{e}_Z$ terms in Eq. (11) describe the retrograde precession of $\hat{\mathbf{m}}$ about the orbit normal, but now with a rate that varies with twice the precession frequency. The triple cross product term varies the obliquity i with the same frequency. Recall that the longitude of the ascending node of the equator on the orbit plane Ω is measured from the perihelion direction. The precession rate is minimal when $\Omega = 0$ or π and maximal when $\Omega = \pm\pi/2$. The former corresponds to the node of the equator plane being parallel to the line of apsides such that at the perihelion, the torque due the axial asymmetry of Mercury (K_2 has C_{22} as a factor.) vanishes. When $\Omega = \pm\pi/2$, the node is perpendicular to the line of apsides, and at perihelion, the long axis is tilted the maximum amount relative to the orbit plane. The torque and hence the averaged precession rate is thus maximal for this phase, since the biggest torque due to the egg shape of Mercury comes at the perihelion when the long axis is tipped above or below the plane of the orbit while still being oriented toward the Sun

as closely as possible because of the spin-orbit resonance. For $\Omega = 0$ or π , the opportunity for the Sun to exert a large torque on the axial asymmetry at perihelion is lost, and so the average of the torque around the orbit is minimal.

The triple product term in Eq. (11) lies along the projection of the spin vector $\hat{\mathbf{m}}$ on the orbit plane. So for $\pi/2 > \Omega > 0$ the obliquity is increasing, whereas it is decreasing for $0 > \Omega > -\pi/2$. Hence, the obliquity has a minimum when the spin is crossing the X axis ($\Omega = \pm\pi/2$) and a maximum when it crosses the Y axis ($\Omega = 0$ or π). The precession rate is maximal when the obliquity is minimal and *vice versa*, and the precession path of the spin is elliptical with the long axis along the Y axis. The reader will notice that there is also a component of the triple vector product torque that is parallel to $\hat{\mathbf{m}}$. This component may not be real because of the approximations involved in arriving at Eq. (9), but if it is real, there may be a displacement of the center of physical libration as a function of precessional phase.

A good approximation to the precessional motion can be obtained by neglecting the last term in Eq. (9), since it is $O(i^2)$ smaller than the next smallest term. With $\hat{\mathbf{m}} = \sin i \sin \Omega \mathbf{e}_x - \sin i \cos \Omega \mathbf{e}_y + \cos i \mathbf{e}_z$, we can write Eq. (9) in still another way with a rearrangement of terms,

$$\begin{aligned} \frac{\langle \vec{N} \rangle}{C_m \dot{\psi}_m} &= \left[K_1 m_z + K_3(1 - m_z) - K_2 \frac{(1 + m_z)}{2} \right] m_y \mathbf{e}_x \\ &\quad - \left[K_1 m_z + K_3(1 - m_z) + \frac{K_2(1 + m_z)}{2} \right] m_x \mathbf{e}_y, \end{aligned} \quad (13)$$

where $m_{x,y,z}$ are the respective components of $\hat{\mathbf{m}}$. Then

$$\frac{d\hat{\mathbf{m}}}{dt} = \frac{\langle \vec{N} \rangle}{C_m \dot{\psi}_m},$$

where $\dot{\psi}_m \equiv 1.5n$ is fixed by the spin orbit resonance and can be removed from the time derivative. From Eq. (13)

$$\begin{aligned} \frac{dm_x}{dt} &= \left[K_1 m_z + K_3(1 - m_z) - K_2 \frac{(1 + m_z)}{2} \right] m_y \\ \frac{dm_y}{dt} &= - \left[K_1 m_z + K_3(1 - m_z) + K_2 \frac{(1 + m_z)}{2} \right] m_x, \end{aligned} \quad (14)$$

where for small obliquity, with $m_z \approx 1$, the solution is

$$\begin{aligned} m_x &= m_x^0 \cos \left[\left(\sqrt{K_1^2 - K_2^2} \right) t + \zeta \right] \\ m_y &= \sqrt{\frac{K_1 + K_2}{K_1 - K_2}} m_x^0 \sin \left[\left(\sqrt{K_1^2 - K_2^2} \right) t + \zeta \right], \end{aligned} \quad (15)$$

where m_x^0 and ζ are constants depending on initial conditions. With $C_m = 0.18M_M R^2$, $\dot{\psi} = 1.5n$, $J_2 = 6 \times 10^{-5}$, and $C_{22} = 1 \times 10^{-5}$ (Anderson *et al.* 1987), $K_1 = 1.117 \times 10^{-2}$ rad/yr and $K_2 = 8.391 \times 10^{-5}$ rad/yr, the precession period of Mercury’s spin about the orbit normal (or the Cassini state) is 562 years. If $C_m = 0.16M_M R^2$, the precession period would be reduced to 500 years. If the core were solid and $C = 0.33M_M R^2$, the precession period would be 1031 years. This compares to a 1066 year period obtained numerically by Rambaux and Bois (2004). The ratio of the axes of the ellipse traced out by the projection of the spin vector on the orbit plane is $m_Y^{max}/m_X^{max} = \sqrt{(K_1 + K_2)/(K_1 - K_2)} = 1.0075$. This solution is consistent with the deductions about the precession from Eq. (11) discussed above.

2.2. Tidal Torque

The tidal torque is given by

$$\vec{T} = \frac{3k_2 GM_\odot^2 R^5}{r^6} (\hat{\mathbf{r}} \cdot \hat{\mathbf{r}}_T) (\hat{\mathbf{r}}_T \times \hat{\mathbf{r}}), \quad (16)$$

where k_2 is the second degree potential Love number, $\hat{\mathbf{r}}$ is a unit vector toward the Sun, and $\hat{\mathbf{r}}_T$ is a unit vector toward the tidal maximum, which is the sub-Sun position on Mercury a short time Δt in the past.

$$\hat{\mathbf{r}}_T = \hat{\mathbf{r}} - \frac{d\hat{\mathbf{r}}}{dt} \Delta t, \quad (17)$$

where the time derivative is relative to the body system of coordinates. Replacement of $\hat{\mathbf{r}}_T$ with Eq. (17) yields

$$\vec{T} = \frac{3k_2 GM_\odot^2 R^5 \Delta t}{r^6} \hat{\mathbf{r}} \times \dot{\hat{\mathbf{r}}}, \quad (18)$$

where we have set $\hat{\mathbf{r}} \cdot \hat{\mathbf{r}}_T = 1$. So with the generic relation for a vector \vec{D} , $(d\vec{D}/dt)_{body} = (d\vec{D}/dt)_{space} - \vec{\omega} \times \vec{D}$, and with $\vec{D} \rightarrow \hat{\mathbf{r}} = \cos f \mathbf{e}_X + \sin f \mathbf{e}_Y$ and $\vec{\omega} \rightarrow \dot{\psi}_m (\sin i \sin \Omega \mathbf{e}_X - \sin i \cos \Omega \mathbf{e}_Y + \cos i \mathbf{e}_Z) + \dot{\Omega} \mathbf{e}_Z$, it is easy to obtain

$$\begin{aligned} \hat{\mathbf{r}} \times \dot{\hat{\mathbf{r}}} &= \dot{\psi}_m \sin i \cos(f - \Omega) (-\sin f \mathbf{e}_X + \cos f \mathbf{e}_Y) \\ &\quad + (\dot{f} - \dot{\Omega} - \dot{\psi}_m \cos i) \mathbf{e}_Z \end{aligned} \quad (19)$$

Eq. (19) is substituted into Eq. (18) and averaged over the orbit period. Useful averages are

$$\begin{aligned} \left\langle \frac{a^6}{r^6} \dot{f} \right\rangle &= n \left(1 + \frac{15}{2} e^2 + \frac{45}{8} e^4 + \frac{5}{16} e^6 \right) / (1 - e^2)^6 = n f_1(e) \\ \left\langle \frac{a^6}{r^6} \right\rangle &= \left(1 + 3e^2 + \frac{3}{8} e^4 \right) / (1 - e^2)^{9/2} = f_2(e) \\ \left\langle \frac{a^6}{r^6} \cos 2f \right\rangle &= \left(\frac{3}{2} e^2 + \frac{1}{4} e^4 \right) / (1 - e^2)^{9/2} = f_3(e) \end{aligned}$$

$$\begin{aligned}\left\langle \frac{a^6}{r^6} \cos^2 f \right\rangle &= \frac{f_2(e) + f_3(e)}{2} \\ \left\langle \frac{a^6}{r^6} \sin^2 f \right\rangle &= \frac{f_2(e) - f_3(e)}{2}\end{aligned}\quad (20)$$

where $\dot{f} = n(a^2\sqrt{1-e^2})/r^2$ has been used in the first of Eqs. (20). The averaged tidal torque is thus

$$\begin{aligned}\langle \vec{T} \rangle &= \frac{3k_2GM_\odot^2R^5\Delta t}{a^6} \left\{ -\dot{\psi}_m \sin i \sin \Omega \left(\frac{f_2(e) - f_3(e)}{2} \right) \mathbf{e}_x \right. \\ &\quad \left. + \dot{\psi}_m \sin i \cos \Omega \left(\frac{f_2(e) + f_3(e)}{2} \right) \mathbf{e}_y \right. \\ &\quad \left. + [nf_1(e) - f_2(e)\dot{\psi}_m \cos i] \mathbf{e}_z \right\},\end{aligned}\quad (21)$$

where we have neglected $\dot{\Omega}$ compared to n and $\dot{\psi}_m$.

The relationship between the dissipation function Q and Δt follows from a simple example. The dissipation parameter Q for an system oscillating at frequency ω is defined by (e.g. Lambeck, 1980 p 14)

$$\frac{1}{Q} = \frac{\oint \frac{dE}{dt} dt}{2\pi E^*} = \omega \Delta t, \quad (22)$$

where the numerator is the energy dissipated during a complete cycle of oscillation and E^* is the maximum energy stored during the cycle. For a tidally distorted, nearly spherical body with the disturbing body in a circular equatorial orbit, a cycle would consist of half a rotation of the distorted body relative to the body causing the tide. For a complex tide generated by a non circular, non equatorial orbit of the disturbing body, each periodic term in a Fourier decomposition of the tide would have its own maximum stored energy and dissipation over a complete cycle of oscillation.

The response of an oscillator with forcing function $F = A' \sin \omega t$ when $\omega \ll \omega_0$, with ω_0 being the lowest frequency of free oscillation, can be represented by $x = B' \sin \omega(t - \Delta t)$, where Δt is the phase lag in the response due to the dissipation as was assumed above for the tidal response. The rate at which the forcing function does work is $dE/dt = F\dot{x} = A'B'\omega \sin \omega t \cos \omega(t - \Delta t)$. Then

$$E(t) = \int_{t_1}^t F\dot{x} dt = A'B'\omega \left[\frac{-\cos(2\omega t - \omega\Delta t)}{4\omega} + \frac{\sin \omega\Delta t}{2} t \right]_{t_1}^t. \quad (23)$$

The first term in Eq. (23) is the periodic storage of energy in the oscillator, and the second is the secular loss of energy. The maximum energy stored is just twice the coefficient of the cosine term, $E^* = A'B'/2$, and the energy dissipated during a complete period of $2\pi/\omega$ is $\Delta E = A'B'\pi\omega\Delta t$ with $\sin \omega\Delta t \approx \omega\Delta t$. We use the energy stored as the energy increment

above the minimum energy in the first term since the stored tidal energy will always be an increase over the relaxed spherical shape of the body. Hence $1/Q = \omega\Delta t$ as indicated in Eq. (22). Since Δt is independent of frequency, Q is inversely proportional to frequency in this model. For Earth like materials, Q is almost independent of frequency for a wide range of frequencies above typical tidal frequencies (Knopoff, 1964), but to avoid a step function reversal in torque when a tidal frequency changes sign, it is not unlikely that the above frequency dependence will prevail for the small tidal frequencies.

$Q = 100$ is typical of Earth-like materials (Knopoff, 1964) and apparently for Phobos generated tides on Mars (Smith and Born, 1976). For Mars the dominant frequency is $\omega = 2(\dot{\psi} - n_P)$, where $\dot{\psi}$ is Mars rotational angular velocity and n_P is Phobos' mean orbital motion. The factor 2 follows from there being two tidal cycles for each synodic period. With a rotation period of $24^h37^m23^s$ and an orbital period of 0.319 days, $\omega = 3.14 \times 10^{-4}$ rad/s leading to $\Delta t \approx 32$ seconds for $Q = 100$. For Mercury, the fundamental tidal period is the orbit period, since Mercury rotates 180° relative to the Sun for each orbit. Although one might infer that Q is inversely proportional to frequency near a particular frequency to smooth the transition from positive to negative frequency, it cannot be the case that the same proportionality constant will apply over a very wide range of frequency as indicated by $Q \approx 100$ nearly independent of frequency between approximately 10 and 10^6 cps for Earth materials (Knopoff, 1964). We can write $\Delta t = P/(2\pi Q_0)$, with Q_0 being the value appropriate to the 88 day orbital period P .

2.3. Damping the Obliquity

To evaluate the damping of the free precession, or equivalently, the rate of change of the obliquity i of the mantle due to the torques on the right hand side of the first of Eqs. (5), we write $\cos i = \mathbf{e}_o \cdot \hat{\mathbf{m}}$. (Recall $\mathbf{e}_o = \mathbf{e}_z$.) With $\vec{\beta} = C_m \dot{\psi}_m = C_m \dot{\psi}_m \hat{\mathbf{m}}$,

$$\frac{d \cos i}{dt} = \frac{d}{dt} \left(\frac{\mathbf{e}_o \cdot \vec{\beta}}{\beta} \right) = \frac{1}{\beta} \left(\mathbf{e}_o \cdot \frac{d\vec{\beta}}{dt} \right) - \frac{1}{\beta^2} (\mathbf{e}_o \cdot \vec{\beta}) \frac{d\beta}{dt}. \quad (24)$$

If we note that $d\vec{\beta}/dt = \vec{\mathcal{T}}$, where $\vec{\mathcal{T}}$ is the total torque acting on the mantle, and that $d\beta/dt = \hat{\mathbf{m}} \cdot \vec{\mathcal{T}}$, Eq. (24) becomes

$$\frac{d \cos i}{dt} = [\mathbf{e}_o - (\mathbf{e}_o \cdot \hat{\mathbf{m}})\hat{\mathbf{m}}] \cdot \frac{\vec{\mathcal{T}}}{\beta} = \sin i \frac{\mathbf{e}_\perp \cdot \vec{\mathcal{T}}}{\beta}, \quad (25)$$

where \mathbf{e}_\perp is a unit vector lying in the equator plane that is perpendicular to the node of the equator on the orbit plane.

From Eqs. (11) and (25),

$$\sin i \frac{\mathbf{e}_\perp \cdot \langle \vec{N} \rangle}{\beta} = -K_2 \sin^2 i \cos i \sin 2\Omega, \quad (26)$$

represents the periodic variation in the obliquity during the precession. From Eqs. (21) and with $\mathbf{e}_\perp = -\cos i \sin \Omega \mathbf{e}_x + \cos i \cos \Omega \mathbf{e}_y + \sin i \mathbf{e}_z$,

$$\sin i \frac{\mathbf{e}_\perp \cdot \langle \vec{T} \rangle}{\beta} = K_4 \sin^2 i \left[n f_1(e) - \frac{\dot{\psi}_m \cos i}{2} (f_2(e) - f_3(e) \cos 2\Omega) \right], \quad (27)$$

where

$$K_4 = \frac{3k_2 GM_\odot^2 R^5}{n Q_0 C_m \dot{\psi}_m a^6}, \quad (28)$$

with $1/nQ_0$ replacing Δt as described above. The functions $f_i(e)$ are defined in Eqs. (20) with $f_1(e) = 1.72$, $f_2(e) = 1.37$, and $f_3(e) = 0.0779$ for $e = 0.206$.

We have only the core-mantle interaction term left to evaluate, which we determine with the analysis of Goldreich and Peale (1970). We note first that $K_2 \ll K_1$ from Eqs. (12), and since the tidal torque and core-mantle interaction are small compared to \vec{N} , the zero-order solution of Eqs. (5) is approximately a uniform retrograde precession of the spin vector at the rate $-\dot{\Omega}$, where $\dot{\Omega}$ is the magnitude of the motion of the projection of the spin vector on the orbit plane. This zero order motion of the mantle is determined from Eq. (13)

$$\frac{d\hat{\mathbf{m}}}{dt} \approx K_1 (\hat{\mathbf{m}} \times \mathbf{e}_o) = K_1 \sin i (-\cos \Omega \mathbf{e}_x - \sin \Omega \mathbf{e}_y), \quad (29)$$

where we have also omitted the K_3 term because of the factor $1 - m_z \approx 0$. From Eq. (29)

$$\dot{\Omega} = K_1 = \frac{2\pi}{562} \text{yr}^{-1}, \quad (30)$$

where the 562 year precession period is discussed above for $C_m = 0.18 M_M R^2$. If we substitute Eq. (30) into Eq. (29), restore the core-mantle interaction but continue to ignore the tidal torque, and divide both equations by $C_m \dot{\Omega}^2$ to make them dimensionless, we can write

$$\begin{aligned} \frac{d\dot{\psi}'_m}{dt'} &= \dot{\psi}'_m (\hat{\mathbf{m}} \times \mathbf{e}_o) - k' (\dot{\psi}'_m - \dot{\psi}'_c) \\ \frac{d\dot{\psi}'_c}{dt'} &= \frac{k'}{C'} (\dot{\psi}'_m - \dot{\psi}'_c) \end{aligned} \quad (31)$$

where $t' = \dot{\Omega} t$, $\dot{\psi}'_{m,c} = \dot{\psi}_{m,c} / \dot{\Omega}$, $k' = k / (C_m \dot{\Omega})$, and $C' = C_c / C_m$. With $\vec{\delta}' = \dot{\psi}'_m - \dot{\psi}'_c$, we can write

$$\frac{d\vec{\delta}'}{dt'} = \dot{\psi}'_m (\hat{\mathbf{m}} \times \mathbf{e}_o) - k' \left(\frac{C' + 1}{C'} \right) \vec{\delta}'. \quad (32)$$

If we assume $t' = 0$ when $\Omega = 0$ (*i.e.* with the ascending node of the equator plane on the orbit plane aligned with the perihelion direction), we can write $\Omega = -\dot{\Omega} t = -t'$ and

replace Ω in the inertial system representation of $\hat{\mathbf{m}} \times \mathbf{e}_o$ in Eq. (29) with $-t'$. Then

$$\begin{aligned}\frac{d\delta'_x}{dt'} + \alpha\delta'_x &= -\dot{\psi}'_m \sin i \cos t', \\ \frac{d\delta'_y}{dt'} + \alpha\delta'_y &= \dot{\psi}'_m \sin i \sin t', \\ \frac{d\delta'_z}{dt'} + \alpha\delta'_z &= 0,\end{aligned}\tag{33}$$

where $\alpha = k'(C' + 1)/C'$ and $\delta'_{x,y,z}$ are the components of $\vec{\delta}'$ along the respective coordinate axes. The solutions of these equations are

$$\begin{aligned}\delta'_x &= A_1 \exp -\alpha t' + \dot{\psi}'_m \sin i \left(\frac{-\alpha \cos t' - \sin t'}{\alpha^2 + 1} \right), \\ \delta'_y &= A_2 \exp -\alpha t' + \dot{\psi}'_m \sin i \left(\frac{-\cos t' + \alpha \sin t'}{\alpha^2 + 1} \right), \\ \delta'_z &= A_3 \exp -\alpha t',\end{aligned}\tag{34}$$

where A_i are constants determined by initial conditions.

With $\mathbf{e}_\perp = -\cos i \sin \Omega \mathbf{e}_x + \cos i \cos \Omega \mathbf{e}_y + \sin i \mathbf{e}_z$, and $\Omega = -t'$, we substitute the steady state solution for $\vec{\delta}'$ into the normalized form of Eq. (25), with

$$\left\langle -\frac{k' \sin i}{\dot{\psi}'_m} \vec{\delta}' \cdot \mathbf{e}_\perp \right\rangle = \frac{k' \sin^2 i \cos i}{\alpha^2 + 1},\tag{35}$$

to yield in dimensionless form

$$\begin{aligned}\frac{d \cos i}{dt'} &= \sin i \left(\frac{K_2}{K_1} \sin i \cos i \sin 2t' + \frac{k' \sin i \cos i}{\alpha^2 + 1} \right) \\ &+ K_4 \sin^2 i \left\{ n' f_1(e) - \frac{\dot{\psi}'_m \cos i}{2} [f_2(e) + f_3(e) \cos 2t'] \right\},\end{aligned}\tag{36}$$

where $n' = n/\dot{\Omega}$. If we average Eq. (36) over a precession period, the circular functions with t' in their arguments vanish. Next with $d \cos i / dt' = -\sin i di / dt'$ and setting $\sin i \approx i$ and $\cos i \approx 1$, we arrive at

$$\left\langle \frac{di}{dt'} \right\rangle = -i \left[\frac{k'}{\alpha^2 + 1} + K_4 \left(n' f_1(e) - \frac{\dot{\psi}'_m}{2} f_2(e) \right) \right].\tag{37}$$

The time constant for the decay of the obliquity due to both a core-mantle interaction and tidal dissipation is the reciprocal of the coefficient of i in Eq. (37).

We relate the coupling constant k' to the core viscosity by equating the time scale for the spin-up of a viscous liquid in a closed container with the time scale for relaxation of the

differential rotation. From Eqs. (34), the dimensioned time scale in the transient part of $\dot{\delta}'_i$ is

$$\tau_\delta = \frac{1}{\alpha \dot{\Omega}} = \frac{C'}{(1 + C')k' \dot{\Omega}} = \frac{R_c}{(\dot{\psi}_m \nu)^{1/2}}, \quad (38)$$

where the expression on the right is the time scale for a fluid with kinematic viscosity ν , rotating differentially in a closed spherical container with radius R_c , to become synchronously rotating with the container at angular velocity $\dot{\psi}_m$ (Greenspan and Howard, 1963). Here $\dot{\psi}_m = 1.5n$, $R_c = 0.75R$ is Mercury's core radius (Siegfried and Solomon, 1987), $\dot{\Omega} = (2\pi/562) \text{ yr}^{-1}$ and $C' = C_c/C_m \approx 1$. So

$$k' = \frac{C'(\dot{\psi}_m \nu)^{1/2}}{(1 + C')\dot{\Omega}R_c} = 8.59 \times 10^{-3} \nu^{1/2}, \quad (39)$$

where ν is expressed in cm^2/sec .

The kinematic viscosity of the Earth's core has been estimated from first principles to lie within the bounds $4.5 \times 10^{-3} \lesssim \nu \lesssim 4.1 \times 10^{-2} \text{ cm}^2/\text{sec}$ by Wijs *et al.* (1998). If we choose $\nu = 0.01 \text{ cm}^2/\text{sec}$, then $\alpha = 2k' = 1.72 \times 10^{-3}$, and its square can be neglected in the denominator of the first term on the right of Eq. (37). With $P = 88$ days, $R = 2439$ km, $C_m = 0.18M_M R^2$, $M_M = 3.302 \times 10^{26}$ g, the time scale for damping Mercury's free precession becomes

$$\tau_{prec} = \frac{89 \text{ years}}{8.59 \times 10^{-3} \nu^{1/2} + 8.08 \times 10^{-3} k_2/Q_0}. \quad (40)$$

Theoretical values of Mercury's $k_2 \approx 0.3$ to 0.4 (Spohn *et al.* 2001; Van Hoolst and Jacobs, 2003), and $Q_0 \approx 100$ is typical for Mars and Earth (Smith and Born, 1976; Knopoff, 1964) such that $k_2/Q_0 = 0.004$ is a plausible value. With $\nu = 0.01 \text{ cm}^2/\text{sec}$, we find $\tau_{prec} \approx 1.00 \times 10^5$ years under the action of both tidal dissipation and core mantle interaction, and $\tau_{prec} = 1.04 \times 10^5$ years and $\tau_{prec} = 2.76 \times 10^6$ years for core-mantle interaction and tidal dissipation respectively if they acted alone.

The development of Eqs. (5) for numerical integration is given in Appendix A. An advantage of a numerical approach is that the consequences for the damping of large values of ν , where the approximations used above are not valid, can be determined. Since, $\nu \gg 0.01$ is unlikely, we shall not show the damping histories for large ν , but remark that the damping time scale is a minimum for $\nu \approx 1000 \text{ cm}^2/\text{sec}$ where the precession amplitude is nearly critically damped. For larger ν the coupling is sufficiently strong that the core nearly follows the mantle as both precess together and the precession period increases from 562 years to somewhat over 1000 years appropriate for a solid planet. The damping time scale for the precession amplitude is similarly increased from the minimum as ν is increased. The Greenspan and Howard spin-up time scale in Eq. (38) also must be replaced by a viscous time scale for large ν in relating ν to k' .

In Fig. 3 we demonstrate that the same time scale for damping the precession amplitude from the combination of core-mantle and tidal dissipation is obtained numerically

as analytically for the same $\nu = 0.01 \text{ cm}^2/\text{sec}$ and $k_2/Q_0 = 0.004$. If we set $k = 0$, the damping time estimated numerically similarly to Fig. 3 is $\approx 2.8 \times 10^6$ years compared to 2.76×10^6 years determined analytically, which confirms the analytic development. Damping time scales for reasonable choices of ν and k_2/Q_0 are all short compared to the solar system age, so we would expect the free precession to be completely damped, barring excitation by an unspecified mechanism.

[Figure 3]

3. Damping of free libration

The treatment of the libration damping is considerably simpler than that of the precession amplitude as we can assume zero obliquity as well as principal axis rotation. Eqs. (5) still apply, but are now scalar equations since there are only torques about the Z axis, which is now coincident with the z axis. With $\hat{\mathbf{r}} \times \dot{\hat{\mathbf{r}}} = -(\dot{\psi}_m - \dot{f})\mathbf{e}_z$, we can write

$$\begin{aligned} C_m \ddot{\psi}_m &= N + T - k(\dot{\psi}_m - \dot{\psi}_c), \\ &= -\frac{3}{2}(B - A)\frac{GM_\odot}{r^3} \sin 2\xi - \frac{3k_2 GM_\odot^2 R^5}{r^6 Q_0} \left(\frac{\dot{\psi}_m - \dot{f}}{n} \right) - k(\dot{\psi}_m - \dot{\psi}_c), \\ C_c \ddot{\psi}_c &= k(\dot{\psi}_m - \dot{\psi}_c), \end{aligned} \quad (41)$$

where $C_{22} = (B - A)/(4M_M R^2)$ has been used. The relations between f , ϕ , ξ , and ψ_m are shown in Fig. 4, where the X axis is now drawn from the Sun to the perihelion with line SM drawn from the Sun to Mercury. The angles are linked to the orbital motion through $\psi_m = \xi + f$, where f is the true anomaly.

[Figure 4]

Mercury’s rotation deviates from $\dot{\psi}_m = 1.5n$ by only a small amount, where $\dot{\psi}_m$ is the magnitude of $\dot{\vec{\psi}}_m$. We therefore write $\dot{\gamma}_m = \dot{\psi}_m - 1.5n$ as the deviation of the spin from the mean value. The angular deviation of, say, Mercury’s axis of minimum moment of inertia (“long axis”) from the position it would have had if the rotation were uniform is then $\gamma_m = \psi_m - 1.5M$, where $M = nt$ is the mean anomaly. γ_m is thus the angle between Mercury’s long axis and the direction to the Sun when Mercury is at perihelion. The equation of rotational motion for the mantle becomes

$$\ddot{\gamma}_m + \frac{3}{2}n^2 \frac{B - A}{C_m} \frac{a^3}{r^3} \sin(2\gamma_m + 3M - 2f) = \frac{T}{C_m} - \frac{k}{C_m}(\dot{\gamma}_m - \dot{\gamma}_c), \quad (42)$$

where $n^2 = GM_\odot/a^3$ is used, with a being the orbit semimajor axis. The expansion of $\sin(2\gamma_m + 3M - 2f)$ leads to factors $(a^3/r^3) \sin 2f$ and $(a^3/r^3) \cos 2f$, which when expanded in terms of the mean anomaly M with the help of Cayley’s tables (1859) gives

$$\ddot{\gamma}_m + 3 \frac{B - A}{C_m} G_{201}(e) \gamma_m = -\frac{3}{2} \frac{B - A}{C_m} \left[\left(1 - 11e^2 + \frac{959}{48}e^4 + \dots \right) \sin t \right]$$

$$\begin{aligned}
 & - \left(\frac{1}{2}e + \frac{421}{48}e^3 + \dots \right) \sin 2t + \dots \Big] \\
 & + \frac{T}{C_m n^2} - \frac{k}{C_m n} \left(\frac{\dot{\gamma}_m}{n} - \frac{\dot{\gamma}_c}{n} \right), \tag{43}
 \end{aligned}$$

where e is the orbital eccentricity, $G_{201}(e) = 7e/2 - 123e^3/16 + \dots$ is a Kaula (1966) eccentricity function. We have made the equation dimensionless by dividing by n^2 and letting $nt = M \rightarrow t$. Also, $\sin 2\gamma_m \rightarrow 2\gamma_m$, $\cos 2\gamma_m \rightarrow 1$ have been used, and a Fourier series in t multiplied by γ_m has been omitted from the right hand side of the equation, since it is so much smaller than the unit coefficient of the displayed series.

If we neglect the weak tidal and core-mantle torques for the moment, Eq.(43) is a simple forced harmonic oscillator equation describing the free and forced librations of longitude for Mercury. The amplitude of the $\sin 2t$ term is about 11% of that of the $\sin t$ term and higher order terms are even less. Since the overall amplitude of the physical libration is not changed by this second term in the series, and higher order terms contribute negligibly, we retain only the $\sin t$ in defining the amplitude of the physical libration in Eq. (2). Although this truncation of the series gives a reasonably good approximation to the physical libration angle, it gives a poor representation of the deviation of the angular velocity from the mean value. This is shown in Fig. 5 where the flat tops on the angular velocity curve at perihelion result from the fact that the orbital angular velocity is close to the spin angular velocity near perihelion, and with the long axis nearly aligned with the direction to the Sun during this time, the torque on the axial asymmetry is nearly zero. A detailed explanation of the behavior of $d\psi_m/dt$ near the perihelion is given in Appendix B.

[Figure 5]

The free libration is treated by averaging Eq. (43) over an orbit period such that the periodic terms responsible for the physical libration vanish. T is replaced by its averaged value $\langle T \rangle$ and $\dot{\gamma}_m$ and $\dot{\gamma}_c$ are uniform on the orbital time scale. We have already specified the form of the frequency dependent tidal torque in Eqs. (41), where Δt (defined in Eq. (17)) is expressed in terms of $\dot{\psi}_m - \dot{f}$.

$$\begin{aligned}
 \langle T \rangle &= \frac{1}{2\pi} \int_0^{2\pi} T dM, \\
 &= -\frac{3k_2 n^4 R^5}{2\pi G Q_0 \sqrt{1-e^2}} \int_0^{2\pi} \frac{a^4}{r^4} \left(\frac{3}{2} + \frac{\dot{\gamma}_m}{n} - \frac{a^2}{r^2} \sqrt{1-e^2} \right) df, \\
 &= -F \left(V + \frac{\dot{\gamma}_m}{n} \right), \tag{44}
 \end{aligned}$$

where we have used the second form of the mantle equation in Eqs. (41), $dM/df = r^2/(a^2\sqrt{1-e^2})$, $\dot{f} = na^2\sqrt{1-e^2}/r^2$, and where

$$F = \frac{3k_2 n^4 R^5}{G Q_0 (1-e^2)^{9/2}} \left(1 + 3e^2 + \frac{3}{8}e^4 \right) = \frac{3k_2 n^4 R^5}{G Q_0} f_2(e)$$

$$V = \frac{3}{2} - \frac{(1 + 15e^2/2 + 45e^4/8 + 5e^6/16)}{(1 - e^2)^{3/2}(1 + 3e^2 + 3e^4/8)} = \frac{3}{2} - \frac{f_1(e)}{f_2(e)},$$

which agrees with Eq. (24) of Goldreich and Peale (1966), except for the correction of the coefficient of e^6 from $3/16$ to $5/16$.

We divide Eq. (43) by $x^2 = 3(B - A)G_{201}(e)/C_m$ and further normalize time by $xt = t'$. Time $t \rightarrow t'$ is now normalized by the free libration frequency instead of the precession frequency $\dot{\Omega}$ as in Section 2. The average of Eq. (43) then becomes

$$\begin{aligned} \frac{d^2\gamma'_m}{dt'^2} + \gamma'_m &= -k'(\dot{\gamma}'_m - \dot{\gamma}'_c) - F'(V + x\dot{\gamma}'_m) \\ \frac{d^2\gamma'_c}{dt'^2} &= \frac{k'}{C'}(\dot{\gamma}'_m - \dot{\gamma}'_c), \end{aligned} \quad (45)$$

where $F' = F/C_m x^2 n^2$, $k' = k/C_m x n$, $C' = C_c/C_m$ and $\dot{\gamma}'_{m,c} = \dot{\gamma}_{m,c}/xn$. Similar to the treatment of the precession, the fact that the tidal and core-mantle torques on the mantle are small means that the mantle will librate almost as it would if k and F were zero. We follow the same procedure as in Section 2 but now in scalar form. The zero order solution of the first of Eqs. (45) is then $\gamma_m = \dot{\gamma}'_{m0} \sin t'$ and $\dot{\gamma}'_m = \dot{\gamma}'_{m0} \cos t'$, where $(\gamma_m, \dot{\gamma}'_m) = (0, \dot{\gamma}'_{m0})$ when $t' = 0$. Subtracting the second of Eqs. (45) from the first yields an equation for $\delta = \dot{\gamma}'_m - \dot{\gamma}'_c$.

$$\frac{d\delta}{dt'} + k' \frac{1 + C'}{C'} \delta = -\dot{\gamma}'_{m0} \sin t' - F'(V + x\dot{\gamma}'_{m0} \cos t'), \quad (46)$$

where we have substituted the zero order solutions for γ_m and $\dot{\gamma}'_m$ on the right. Now $F' = 1.5 \times 10^{-2} k_2/Q_0$, where we have used $x = \sqrt{3(B - A)(7e/2 - 123e^3/16)/C_m} = 0.0262$, $C_m = 0.18M_M R^2$, inferred from Siegfried and Solomon (1974), $(B - A)/C_m = 3.5 \times 10^{-4}$, and Mercury's mass $M_M = 3.302 \times 10^{26}$ g. The coefficient of $\cos t'$ in Eq. (46) is a factor of 3.9×10^{-4} less than the coefficient of $\sin t'$ so we can neglect the former term. We keep the constant term leading to the solution

$$\dot{\delta} = A_4 \exp(-\alpha t) + \frac{\dot{\gamma}'_{m0}}{1 + \alpha^2} (\cos t - \alpha \sin t) - \frac{F'V}{\alpha}, \quad (47)$$

where $\alpha = k'(1 + C')/C'$ and A_4 is an arbitrary constant.

The steady state solution for $\dot{\delta}$ is substituted back into the first of Eqs. (45) to yield

$$\frac{d^2\gamma'_m}{dt'^2} + \left(\frac{k'}{1 + \alpha^2} + F'x \right) \frac{d\gamma'_m}{dt'} + \left(1 - \frac{k'\alpha}{1 + \alpha^2} \right) \gamma'_m = -\frac{F'V}{1 + C'}, \quad (48)$$

where we have used the zero order solutions, $\gamma'_m = \dot{\gamma}'_{m0} \sin t'$ and $\dot{\gamma}'_m = \dot{\gamma}'_{m0} \cos t'$ in the steady state solution for $\dot{\delta}$ and rearranged terms. Tidal friction displaces the zero point of the libration by $-F'V/(1 + C') = 1.83 \times 10^{-3} k_2/Q_0 = 7.34 \times 10^{-6}$ radians or ~ 1.5 arcsec for $k_2/Q_0 = 0.004$ ($x = 0.0262$, $V = 0.244$). A measure of this displacement would determine k_2/Q_0 for Mercury. (Tidal friction attempts to slow Mercury's spin to a value that is less

than the current $1.5n$, so at perihelion, the axis of minimum moment of inertia is displaced from exact alignment with the Sun ($\gamma_m \equiv 0$) until the averaged torque on the permanent deformation balances the tidal torque and keeps the spin at the resonant rate.)

The time scale τ_{lib} for damping the free libration amplitude is twice the inverse of the coefficient of $\dot{\gamma}_m$ in Eq. (48). The transient part of the expression for δ in Eq. (47) is the same as that for the precession analysis, so the coupling constant k' is related to the kinematic viscosity of the core by Eq. (39), except $\dot{\Omega}$ must be replaced by xn . Then

$$k' = \frac{C'(\dot{\psi}\nu)^{\frac{1}{2}}}{(1 + C')xnR_c} = 1.41 \times 10^{-4}\nu^{\frac{1}{2}}. \quad (49)$$

The dimensioned time scale for damping the free libration is given by

$$\begin{aligned} \tau_{lib} &= \frac{2}{(k'/(1 + \alpha^2) + F'x)xn} \\ &\approx \frac{2}{(k' + F'x)xn} \\ &\approx \frac{2.92 \text{ rmyears}}{(1.41 \times 10^{-4}\nu^{1/2} + 3.93 \times 10^{-4}k_2/Q_0)} \end{aligned} \quad (50)$$

from Eq. (48), where $\alpha = 2k'$ is small and its square can be neglected. We again choose $\nu = 0.01 \text{ cm}^2/\text{sec}$ after Wijs *et al.* (1998) along with $k_2/Q_0 = 0.004$ discussed above, we find $\tau_{lib} \approx 1.86 \times 10^5$ years under the action of both tidal dissipation and core mantle interaction, and $\tau_{lib} = 2.07 \times 10^5$ years and $\tau_{lib} = 1.86 \times 10^6$ years for core-mantle interaction and tidal dissipation respectively if they acted alone. Eqs. (41) are numerically integrated in Fig. 6 for $\nu = 0.01 \text{ cm}^2/\text{sec}$ and $k_2/Q_0 = 0.004$, where the short period fluctuations in Fig. 6 are the 88 day forced librations superposed on the free libration. The approximately determined time scale is 1.8×10^5 years, which is close to the analytic value of 1.86×10^5 years. Damping time scales for reasonable choices of ν and k_2/Q_0 are all short compared to the solar system age, so we would expect the free librations to be completely damped, barring excitation by an unspecified mechanism.

[Figure 6]

4. Consequences of Impact

This is an exercise to determine what size impactor would be necessary to generate an observable free libration or free precession. We shall assume Mercury has no free motions prior to the impact, and that there is a complete transfer to Mercury of the entire angular momentum of the impactor relative to the center of mass of Mercury. If the impact ejecta is distributed symmetrically about the point of impact, it will carry away little angular momentum. This approximate conservation of angular momentum allows us to infer that

the angular increment in the amplitude of the precession is simply the component of the impactor angular momentum that is perpendicular to the spin axis divided by the spin angular momentum $C_m \dot{\psi}_m$. The increment in the free libration amplitude follows easily from the parallel component of the impactor angular momentum. We shall assume that a free libration amplitude or free precession amplitude of 0.1 arcmin is detectable.

Generally, an impactor, which can be either a comet or asteroid, will strike at a point with spherical coordinates R, θ, ϕ relative to the body principal axis system with velocity relative to the center of mass of Mercury of $\vec{V} = V_R \mathbf{e}_R + V_\theta \mathbf{e}_\theta + V_\phi \mathbf{e}_\phi$. The angular momentum of the impactor relative to the center of mass of Mercury is given by

$$\vec{L}_I = \vec{R} \times \mathcal{M} \vec{V} = \mathcal{M} R (V_\theta \mathbf{e}_\phi - V_\phi \mathbf{e}_\theta), \quad (51)$$

where \mathcal{M} is the mass of the impactor. With $\mathbf{e}_\phi = -\sin \phi \mathbf{e}_x + \cos \phi \mathbf{e}_y$ and $\mathbf{e}_\theta = \cos \theta \cos \phi \mathbf{e}_x + \cos \theta \sin \phi \mathbf{e}_y - \sin \theta \mathbf{e}_z$, we can write

$$\begin{aligned} \vec{L}_I = & \mathcal{M} R [(-V_\theta \sin \phi - V_\phi \cos \theta \cos \phi) \mathbf{e}_x \\ & + (V_\theta \cos \phi - V_\phi \cos \theta \sin \phi) \mathbf{e}_y \\ & + V_\phi \sin \theta \mathbf{e}_z], \end{aligned} \quad (52)$$

With the increment in Mercury's angular momentum, $\Delta \vec{L}_M = \vec{L}_I$, the components of $\vec{L}_M = \vec{L}_M^0 + \Delta \vec{L}_M$ along \mathbf{e}_x and \mathbf{e}_y indicates that a free wobble has been induced. But that is not all, since the redistribution of mass due to the crater and its ejecta redefines the inertia tensor, so x, y, z are no longer the principal axes. The new axis of maximum moment being offset from the original z axis also contributes to the wobble. The component ΔL_z means $\dot{\psi}_m$ has been incremented thereby creating a free libration in longitude. Transforming \vec{L}_M to the inertial system defines a new direction of the total spin angular momentum which no longer coincides with the Cassini state, which has itself been changed because of the change in the inertia tensor. \vec{L}_M now precesses around the new position of the Cassini state. A random impact thus excites all three free motions (see Peale, 1975 for a more detailed treatment), but how large must the impact be for detectable amplitudes?

First we note that

$$\begin{aligned} L_{I\parallel} &= \mathcal{M} R V_\phi \sin \theta \\ L_{I\perp} &= \mathcal{M} R (V_\theta^2 + V_\phi^2 \cos^2 \theta)^{1/2} \end{aligned} \quad (53)$$

are the components of impactor angular momentum just before impact at coordinates (θ, ϕ) that are parallel and perpendicular to the spin axis. We consider first the excitation of a free libration, which involves only $L_{I\parallel}$. The free libration is characterized by Eq. (43), where we neglect the right hand side to yield a small amplitude pendulum equation, whose frequency of oscillation is $xn = n\sqrt{3(B-A)G_{201}(e)/C_m}$. Recall that $\gamma_m = \psi_m - 1.5M$ is the angular deviation of the x axis from the position it would have had if Mercury were

rotating uniformly at angular velocity $1.5n$. If $\gamma_m = 0$ and $\dot{\gamma}_m = \dot{\gamma}_m^0$ at $t = 0$, the amplitude of the libration is

$$\gamma_m^{max} = \dot{\gamma}_m^0 / \omega_0 = \frac{L_{I\parallel}}{C_m x n}, \quad (54)$$

where the final form assumes that all of the libration amplitude is induced by the impact.

If we set $\gamma_m^{max} = 0.1' = 2.91 \times 10^{-5}$ rad as the minimum observable, choose $V_\phi = 60$ km/sec as a common impact velocity, set $C_m = 0.18 M_M R^2$ as before, choose $(B-A)/C_m = 3.5 \times 10^{-4}$ so that $xn = 0.026n$, and maximize the effect of the collision for a given \mathcal{M} by assuming $\theta = \pi/2$, we find the necessary $\mathcal{M} = 1.51 \times 10^{15}$ g. For a density of 1 g/cm^3 , the radius of the impactor is 0.712 km.

Holsapple (1993) has described a careful development of scaling laws that predict the properties of impact craters from the size and velocity of the impactor and the strength and gravitational acceleration of the body on which the impact occurs. His Eq. (22b) gives the rim radius for large craters where gravity dominates the strength of the materials in controlling the outcome of the crater formation.

$$R_r = 10.14 G'^{-0.17} a'^{0.83} U^{0.34}, \quad (55)$$

where R_r is the rim radius of the crater just after it is formed in meters, G' is the ratio of the gravitational acceleration at the surface of the body to that of the Earth, a' is the radius of the impactor in meters, and U is the velocity in km/sec. Eq. (55) ignores the ratio of the impactor density and surface material density raised to a small fractional power. With Mercury's gravitational acceleration of 363 cm/sec compared to Earth's 980 cm/sec, $a' = 712$ m and $U = V_\phi = 60$ km/sec, we find $R_r = 11.3$ km. For a crater this large, it gets even larger because of slumping of the walls, with the expression for the final crater size in terms of R_r given by Eq. (28a) of Holsapple (1993). This is called a transition from a simple bowl-shaped crater to a complex crater with a shallow floor and central peak.

$$\frac{R_f}{R_r} = 1.02 \left(\frac{R_f}{R_*} \right)^{0.079}, \quad (56)$$

where R_f is the final rim radius, and R_* is the transition radius from simple to complex craters. R_* is a function of the surface gravity with $R_* = 5$ km for Mercury (Pike, 1988) (9.5 km for the Moon and 1.5 km for Earth and Venus). Substitution of this value of R_* into Eq. (56) yields 12.4 km as the rim radius expected for the impact event leading to a 0.1' free libration amplitude for Mercury. This is a minimum value because of the choice of the extreme optimum values of V_ϕ and $\sin \theta$ in Eq. (54). It should be noted that the Holsapple crater radii are for vertical impacts, whereas we have calculated the angular momentum impulse for an almost grazing impact. However, this caveat does not change the conclusion that even the least detectable amplitude of a free libration of 0.1' excited by an impact would leave a more than 20 km diameter pristine scar on the surface of Mercury.

For an impact excitation of the precession, the angular amplitude would be

$$\Delta i = \frac{L_{I\perp}}{C_m \dot{\psi}_m} = \frac{\mathcal{M} V_\theta R}{C_m \dot{\psi}_m}, \quad (57)$$

where we have assumed the impact is along a meridian for simplicity. If $\Delta i = 0.1'$, $V_\theta = 60$ km/sec, and $C_m = 0.18 M_M R^2$, then $\mathcal{M} = 8.72 \times 10^{16}$ g. The impactor radius is then $a' = 2.75$ km for a density of 1 g/cm³. It takes a much more energetic impact to excite an observable free precession than an observable free libration. These numbers, when substituted into Eqs. (55) and (56), yield $R_f = 41.7$ km, and the pristine crater left behind from an impact causing a $0.1'$ increment in the amplitude of the free precession would be more than 80 km in diameter. The fact that the Cassini state itself has shifted slightly because of the redefinition of the inertia tensor would not change the free precession amplitude sufficiently to alter this conclusion.

In Table 1 of Levison and Duncan (1997), the rate of impact of Jupiter family comets on Mercury is given as 8.6×10^{-10} comets/year. These are for comets of absolute magnitude < 9 , which correspond to radii $a' \gtrsim 1$ km (H. Levison, private communication 2005). The collision rate of very long period comets is probably small compared to this rate for the Jupiter family comets. (H. Levison, private communication 2005). More than a billion years would elapse on average between impacts on Mercury of sufficient size to excite a $0.1'$ amplitude of the free libration in longitude, and because the larger impactor required, even more time between excitations of a $0.1'$ amplitude of the free precession. Comparing this time between excitations with the $O(10^5)$ year damping times for the libration and precession amplitudes means collisions almost certainly could not be the cause of any observable free libration or free precession.

5. Summary and Conclusions

The spin orbit resonance of Mercury leads to a 30% reduction of the period of precession of the spin about the Cassini state from a contribution of the C_{22} term, compared to the usually derived precession period depending on J_2 alone. This effect also leads to an elliptical precessional path of the spin, where the ratio of the axes of the ellipse is about 1.0075. There is a slight variation in the precession rate about the elliptical path with the maximum occurring when the separation of the spin from the Cassini state is minimal.

The simultaneous effects of tidal dissipation and a viscous liquid core-solid mantle coupling lead to time scales for damping Mercury's free libration in longitude and free precession of the spin about Cassini state 1 that are near 10^5 years. Because Mercury's liquid core is so large, the time scale for damping the precession amplitude by the core-mantle coupling acting alone is a factor of about 25 smaller than the time scale due to the tides alone for plausible choices of the parameters. For the libration damping, the core-mantle time scale is a factor

of about 10 smaller than that for tidal friction. For all reasonable choices of the parameters, the time scales are short compared with the age of the solar system. So if a free libration or free precession amplitude is found by the radar experiments or by the observations of the MESSENGER or BepiColombo spacecraft, still unspecified recent or ongoing excitation mechanisms must be sought. It is possible that there exist observable forced deviations of the spin axis from the Cassini state. If the forcing terms are identified, the amplitudes and phases of such deviations should be known and should not hinder the identification of the Cassini state obliquity. On the other hand, the forcing terms are likely to be of fairly long period, as is likely if the amplitudes of the deviations from the Cassini state are observable. As such their identity may not be obvious and the Cassini state position could be thereby uncertain until careful numerical integrations mapped such forced motions.

An observable libration amplitude (assumed to be $0.1'$) is much easier to generate by impact than an observable precession. But such impact excitation of either motion is very unlikely, since there is an estimated average time span between impacts of sufficient size of about 10^9 years with current cometary fluxes. Excitation by impact no more than a few damping time scales in the past would leave a fresh crater larger than 20 km diameter for the excitation of an observable amplitude of libration and larger than 80 km diameter for the excitation of an observable precession amplitude. An observable free precession will make the obliquity of the Cassini state, and thereby the determination of $C/M_M R^2$ uncertain. But an observable free libration does not hamper the determination of the physical libration amplitude. If Mercury's core were solid, the term with the kinematic viscosity would vanish in the expressions for the damping times of the precession and libration (Eqs. (40) and (50)). But the resulting damping times due to the tides alone would be longer than these equations would indicate for $\nu = 0$, because the constants would then involve the moment of inertia of the entire planet instead of just that of the mantle.

This analysis applies to other bodies in spin-orbit resonances such as the Moon, the regular satellites of the major planets, and Pluto's satellite Charon. The terms selected from the expansion of the torque expressions by the averaging process would correspond to rotation synchronous with the the orbital mean motions instead of 1.5 times the mean motion used here. There are similar contributions to the rate of precession about the Cassini state from C_{22} , since the synchronous rotation ensures terms involving C_{22} do not average to zero and C_{22} will be comparable to J_2 in magnitude. There are indications that some of these bodies even have liquid layers in their interiors (*e.g.*, Spohn and Schubert, 2003), although Europa would be a special case with a liquid ocean (*e.g.* Greenberg, 2004)

It will be more fun to seek alternative dynamic mechanisms of excitation of observed free motions of Mercury than if no such motions are found. A possible albeit unlikely excitation of libration may lie in a coupling between the torques on the permanent deformation as affected by the spin-orbit resonance and the small obliquity of the Cassini state. Although such a libration would not be “free,” a near resonant forcing frequency could mimic a free

libration. The investigation of such speculation is a future objective.

6. Appendix A: Numerical Integration of the Precession Damping

We want to integrate Eqs. (5) over the precession time scale without following high frequency motions on the orbit or libration time scales. The averaged torque on the permanent deformation $\langle \vec{N} \rangle$ is given in Eq. (9), where we set $\psi_m = \psi_0 + 1.5M$ with $\psi_0 = -\Omega$ to accommodate the conditions of the spin-orbit resonance in the averaging process. The last term of Eq. (9) is of order i^2 smaller than the next smallest term, and it is neglected in Eq. (13) written in terms of the components of the unit vector along the spin axis $\hat{\mathbf{m}}$. It is this latter form of the averaged torque on the permanent deformation that we will use here.

The averaged tidal torque is given by Eq. (21). The component of $\langle \vec{T} \rangle$ parallel to the spin axis is balanced by a slight offset of the axis of minimum moment of inertia from the direction to the Sun at perihelion. However, we have removed that degree of freedom in $\langle \vec{N} \rangle$ by assigning $\psi_0 = -\Omega$ after Eq. (9). In order to avoid a secular change in $\dot{\psi}_m$, we keep only the component of $\langle \vec{T} \rangle$ perpendicular both to the spin vector and to the line of nodes. The unit vector in this direction is \mathbf{e}_\perp defined in Eq. (25). From this last equation, we see that this is the only component of $\langle \vec{T} \rangle$ that affects the obliquity. With $\psi_0 = -\Omega$ and the elimination of the tidal acceleration of the spin, we have eliminated integration over the free libration period leaving only the precession time scale in the calculation. So in place of $\langle \vec{T} \rangle$, we shall use

$$\frac{\langle \vec{T} \rangle \cdot \mathbf{e}_\perp}{C_m \dot{\psi}_m} \mathbf{e}_\perp = K_4 \sin i \left[n f_1(e) - \frac{\dot{\psi}_m \cos i}{2} (f_2(e) - f_3(e) \cos 2\Omega) \right] \times (-\cos i \sin \Omega \mathbf{e}_x + \cos i \cos \Omega \mathbf{e}_y + \sin i \mathbf{e}_z) \quad (58)$$

where K_4 is defined by Eq. (28) with $1/(nQ_0)$ replacing Δt as described in Section 2.2. Inclusion of the $f_3(e)$ part of the bracketed coefficient in Eq. (58) leads to a $\sin i$ in the denominator, which complicates the calculation. However, $f_3(e) \approx 0.056 f_2(e)$ for $e = 0.206$ so its omission will lead to a small error in the motion of the spin axis and an indiscernible error in the damping time scale, With this additional approximation, we arrive at

$$\frac{\langle \vec{T} \rangle \cdot \mathbf{e}_\perp}{C_m \dot{\psi}_m} \mathbf{e}_\perp = K_4 [n f_1(e) - \dot{\psi}_m m_z f_2(e)] [-m_z m_x \mathbf{e}_x - m_z m_y \mathbf{e}_y + (m_x^2 + m_y^2) \mathbf{e}_z], \quad (59)$$

where $m_{x,y,z}$ are the components of the unit vector along the spin axis of the mantle, $\hat{\mathbf{m}}$. With $d(C_m \dot{\psi}_m)/dt = C_m \dot{\psi}_m d\hat{\mathbf{m}}/dt$ where $\dot{\psi}_m = 3n/2 = \text{constant}$, we can average Eq. (5) over an orbit period, insert the averaged expressions $\langle \vec{N} \rangle$ and the component of $\langle \vec{T} \rangle$ parallel \mathbf{e}_\perp from Eqs. (13) and (59), divide by K_1 to make the equations dimensionless, set $K_1 t = t'$ and $k/(C_m K_1) = k'$, and write six scalar equations in six unknowns, $m_{x,y,z}, c_{x,y,z}$, where

$c_{x,y,z}$ are the components of the unit vector parallel to the spin of the core.

$$\begin{aligned}
 \frac{dm_x}{dt'} &= \left[m_z + \frac{K_3}{K_1}(1 - m_z) - \frac{K_2}{K_1} \frac{1 + m_z}{2} \right] m_y \\
 &\quad - \frac{K_4 n}{K_1} \left[f_1(e) - \frac{3}{4} f_2(e) m_z \right] m_z m_x - k'(m_x - c_x), \\
 \frac{dm_y}{dt'} &= - \left[m_z + \frac{K_3}{K_1}(1 - m_z) + \frac{K_2}{K_1} \frac{1 + m_z}{2} \right] m_x \\
 &\quad - \frac{K_4 n}{K_1} \left[f_1(e) - \frac{3}{4} f_2(e) m_z \right] m_z m_y - k'(m_y - c_y), \\
 \frac{dm_z}{dt'} &= \frac{K_4 n}{K_1} \left[f_1(e) - \frac{3}{4} f_2(e) m_z \right] (m_x^2 + m_y^2) - k'(m_z - c_z), \\
 \frac{dc_x}{dt'} &= \frac{k'}{C'} (m_x - c_x), \\
 \frac{dc_y}{dt'} &= \frac{k'}{C'} (m_y - c_y), \\
 \frac{dc_z}{dt'} &= \frac{k'}{C'} (m_z - c_z)
 \end{aligned} \tag{60}$$

are the equations that are integrated numerically and that describe the damping of the precession amplitude due to a core-mantle interaction and tidal dissipation. Here $C' = C_c/C_m$, and we have set $\dot{\psi}_m = 1.5n$ in the term from the tides.

7. Appendix B: Description of torque reversal near perihelion.

This is an explanation of the nearly flat top on $d\dot{\gamma}_m/dt$ in Fig. 5. In this figure there is a local minimum in $\dot{\gamma}_m$ at perihelion and two local maxima at equal times before and after perihelion. The angular acceleration is zero at these extremes and corresponds to the axis of minimum moment of inertia (long axis) of Mercury being aligned with the direction to the Sun. We ignore the slight variation in rotation due to the physical librations in determining the torque on Mercury by assuming it is rotating uniformly with $\dot{\psi}_m = 1.5n$. At perihelion, the long axis is also pointing toward the Sun, but $\dot{f} > \dot{\psi}_m = 1.5n$ at this point in the orbit. The long axis does not keep up with the motion of the Sun in Mercury's sky as Mercury passes perihelion, so it starts to point away from the Sun in the direction of the orbital motion. The angle between the Sun and the long axis continues to grow and reaches a local maximum when $\dot{f} = \dot{\psi}_m$, which occurs when $f = 25.743^\circ$ and $M = 16.777^\circ$, 4.101 days after perihelion passage. The torque on Mercury during this time tends to increase the angular velocity corresponding to the positive slope on $d\dot{\gamma}_m/dt$ in Fig. 5 just after perihelion passage. The increasing slope has an inflection at and starts to decrease after the time when $\dot{f} = \dot{\psi}_m$, which is when the angle between the long axis and the Sun starts to decrease. The slope of the $d\dot{\psi}_m/dt = d\dot{\gamma}_m/dt$ curve reaches zero when the axes are again aligned. To bring the

long axis back into alignment with the Sun after perihelion passage, Mercury must rotate through the same angle as it has moved in its orbit, so that $f = 1.5M$ at the time of the first post perihelion alignment. This corresponds to $f = 44.442^\circ$, $M = 29.628^\circ$ at 7.242 days after perihelion passage. After this time, the long axis points on the other side of the Sun and the angular velocity starts to decrease.

The motion is symmetric with respect to the perihelion passage so the numbers corresponding to the approach to perihelion are the negatives of those above. It is ascertained that Mercury is almost synchronously rotating with its instantaneous orbital motion near the perihelion, during which time the long axis never deviates much from pointing toward the Sun. Hence, $\dot{\gamma}_m$ is almost constant for a time near the perihelion as shown in Fig. 5, with the small deviations from a constant value explained above.

8. Acknowledgements

Thanks are due H. Levison for directing me to his results for the rate of cometary impacts on Mercury, to R. Strom for information on crater morphologies. and to J. Wisdom for reminding me of two relevant papers of my own. Jacques Henrard and an anonymous referee provided useful suggestions that improved the manuscript. This work is supported in part by the Planetary Geology and Geophysics Division of NASA under grant NAG5 11666 and by the MESSENGER mission to Mercury.

9. References

- Anderson, J.D., Colombo, G., Esposito, P.B., Lau, E.L., Trager, T.B. 1987. The mass, gravity field and ephemeris of Mercury. *Icarus* 71, 337-349.
- Anselmi, A., Scoon, G.E.N. 2001. BepiColombo, ESA's Mercury Cornerstone mission. *Planet. Space Sci.* 49, 1409-1420.
- Cayley, A. 1859. Tables of the developments of functions in the theory of elliptic motion, *Mem. Roy. Astron. Soc.* 29, 191-306.
- Colombo, G. 1966. Cassini's second and third laws. *Astron. J.* 71, 891-896.
- Goldreich, P., Peale, S.J. 1966. Spin orbit coupling in the solar system. *Astron. J.* 71, 425-438.
- Goldreich, P., Peale, S.J. 1970. The obliquity of Venus, *Astron. J.* 75, 273-284.
- Greenberg, R. 2004. *Europa The Ocean Moon: Search For An Alien Biosphere*, Springer, Berlin, (Praxis, Chichester, UK).

- Greenspan, H.P., Howard, G.N. 1963. On the time dependent motion of a rotating fluid, *J. Fluid Mech.* 17, 385-404.
- Harder, H., Schubert, G. 2001. Sulfur in Mercury's core? *Icarus* 151, 118-122.
- Holin, I.V. 1988. *Izvestiya Vysshikh Uchebnykh Zavedenii, Radiofizika* 31, 515.
- Holin, I.V. 1992. *Izvestiya Vysshikh Uchebnykh Zavedenii, Radiofizika* 35, 433.
- Holin, I.V. 2003. Spin dynamics of terrestrial planets from Earth-based RSDI, *Met. Planet. Sci.* 38, Supplement, Abstract no. 5003.
- Holsapple, K.A. 1993. The scaling of impact processes in planetary sciences, *Ann. Rev. Earth Planet. Sci.* 21, 333-373.
- Kaula, W.M. 1966. *Theory of Satellite Geodesy; Applications of Satellites to Geodesy*, Blaisdell, Waltham, MA.
- Knopoff, L. 1964. *Q, Rev. Geophys*, 2, 625-660.
- Lambeck, K. 1980. *The Earth's Variable Rotation: Geophysical Causes and Consequences*, Cambridge University Press, Cambridge.
- Levison, H.F. Duncan, M.J. 1997. From the Kuiper Belt to Jupiter-family comets: The spatial distribution of ecliptic comets, *Icarus* 127, 13-32.
- Margot, J.L., Peale, S.J., Slade, M.A., Jurgens, R.F., Holin, I.V., 2003. Mercury interior properties from measurements of librations. Mercury, 25th meeting of the IAU, Joint Discussion 2, 16 July, 2003, Sydney, Australia, meeting abstract. (<http://adsabs.harvard.edu>).
- Peale, S.J. 1969. Generalized Cassini's laws, *Astron. J.* 74, 483-489.
- Peale, S.J. 1974. Possible histories of the obliquity of Mercury, *Astron. J.* 79, 722-744.
- Peale, S.J. 1975. Dynamical consequences of meteorite impacts on the Moon, *J. Geophys. Res.* 80, 4939-4946.
- Peale, S.J. 1976a. Does Mercury have a molten core? *Nature* 262, 765-766.
- Peale, S.J. 1976b. Excitation and relaxation of the wobble, precession and libration of the Moon, *J. Geophys Res.* 81, 1813-1827.
- Peale, S.J. 1981. Measurement accuracies required for the determination of a Mercurian liquid core, *Icarus* 48, 143-145.
- Peale, S.J. 1988. Rotational dynamics of Mercury and the state of its core, In *Mercury*, ed. F. Vilas, C.R. Chapman, M.S. Matthews, U. of Arizona Press, Tucson, 461-493.
- Peale, S.J. Phillips, R.J., Solomon, S.C., Smith, D.E., Zuber, M.T., 2002. A procedure for determining the nature of Mercury's core, *Meteor. Planet. Sci.* 37, 1269-1283.

- Pike, R.J. 1988. Geomorphology of impact craters on Mercury, In Mercury, ed. F. Vilas, C.R. Chapman and M.S. Matthews, U. of Arizona Press, Tucson. 165-273.
- Rambaux, N., Bois, E. 2004. Theory of Mercury's spin-orbit motion and analysis of its main librations, *Astron. Astrophys.* 413, 381-393.
- Reese, C.C., Peterson, P.E. 2002. Thermal evolution of Mercury in the conductive regime and implications for magnetism, *Lun. Planet. Sci. XXXIII*, Abstract 1998.
- Siegfried, R.W., Solomon, S.C. 1974. Mercury: Internal structure and thermal evolution, *Icarus* 23, 192-205.
- Smith, J.C., Born, G.H. 1976. Secular acceleration of Phobos and the Q of Mars, *Icarus* 27, 51-53.
- Solomon, S.C., 20 colleagues 2001. The MESSENGER mission to Mercury: Scientific objectives and implementation, *Planet. Space Sci.* 49, 1445-1465.
- Spohn, T. and Schubert, G. 2003 Oceans in the icy Galilean satellites of Jupiter? *Icarus* 161, 456-467.
- Spohn, T., Sohl, F., Wiczerkowski, K. and Conzelmann, V. 2001 The interior structure of Mercury: What we know, what we expect from BepiColombo, *Planet. Space Sci.* 49, 1561-1570.
- Van Hoolst, T., Jacobs, C. 2003 Mercury's tides and interior structure, *J. Geophys. Res.* 108, 7-(1-16).
- Ward, W.M. 1975. Tidal friction and generalized Cassini's laws in the solar system, *Astron. J.* 80, 64-70.
- Wijs, G.A. de, Kresse, G., Vočadlo, L., Dobson, D., Alfè, D., Gillan, M.J., Price, G.D. 1998. The viscosity of liquid iron at the physical conditions of the Earth's core, *Nature* 392, 805-807.
- Zuber, M.T., Smith, D.E., 1997. Remote sensing of planetary librations from gravity and topography data: Mercury simulation. *Lunar Planet. Sci.* 28, 1637-1638.

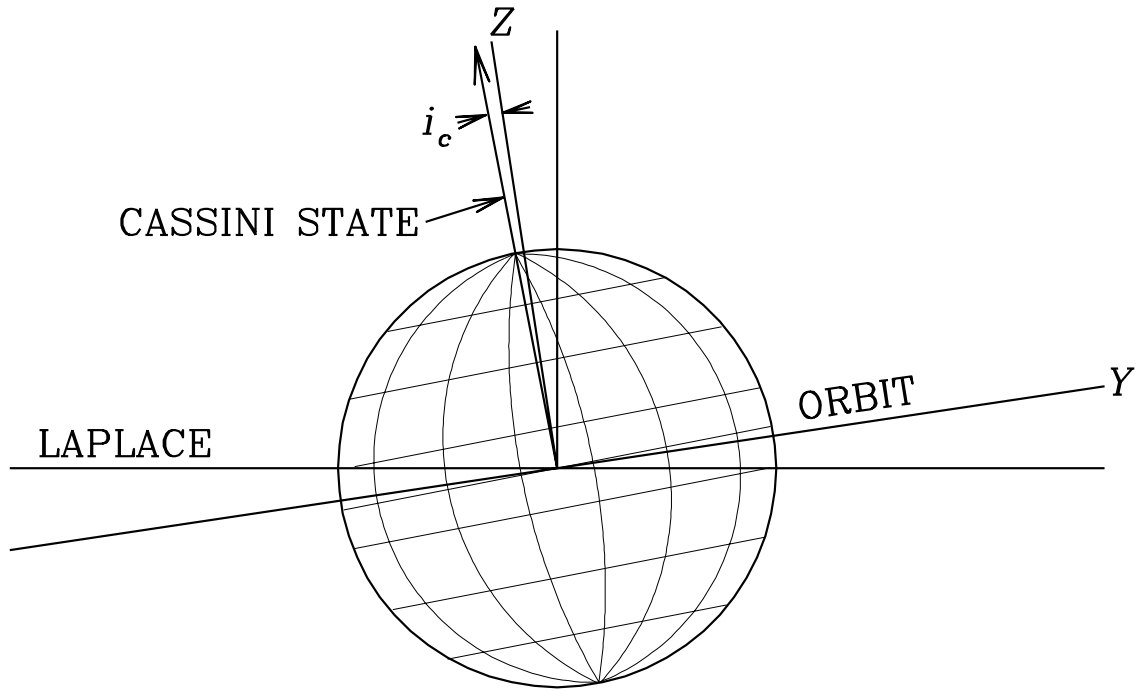


Fig. 1.— Geometry of Cassini state 1. The Z axis is perpendicular to the orbit plane, and the ascending node of the orbit on the Laplace plane and the ascending node of the equator on the orbit plane both coincide with the X axis, which comes out of the paper. The obliquity of the Cassini state is i_c .

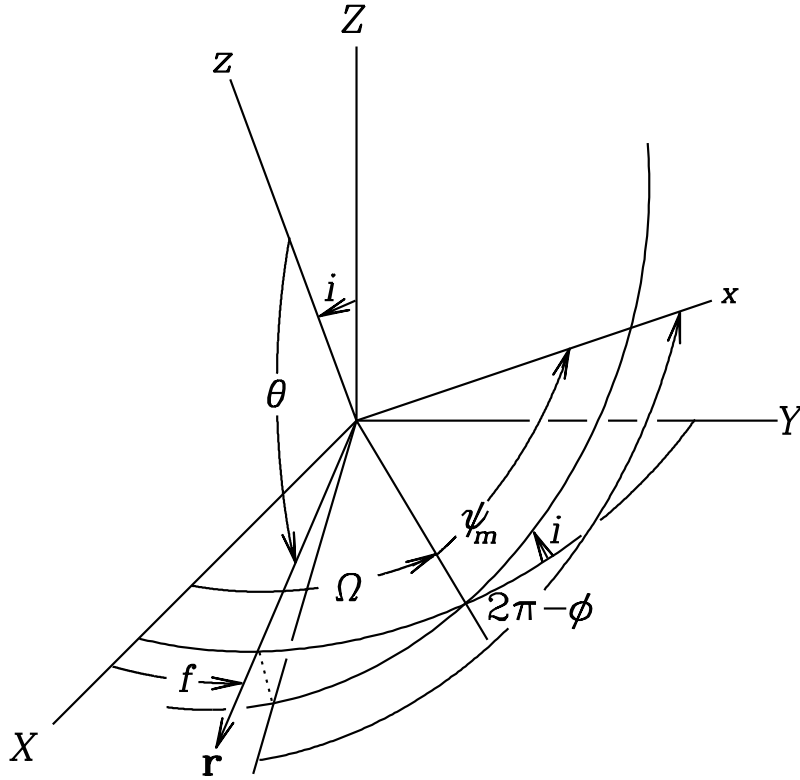


Fig. 2.— Coordinates for describing Mercury's precession. The XY plane is the orbit plane with the X axis pointing toward the perihelion position, Ω is the longitude of the ascending node of the equator plane on the orbit plane, i is the obliquity, and ψ_m locates the x body axis of minimum moment of inertia (of the mantle) relative to the ascending node. The z axis is the axis of maximum moment of inertia, which is also the spin axis. Spherical polar coordinates $r\theta\phi$ locate the Sun relative to the body axes.

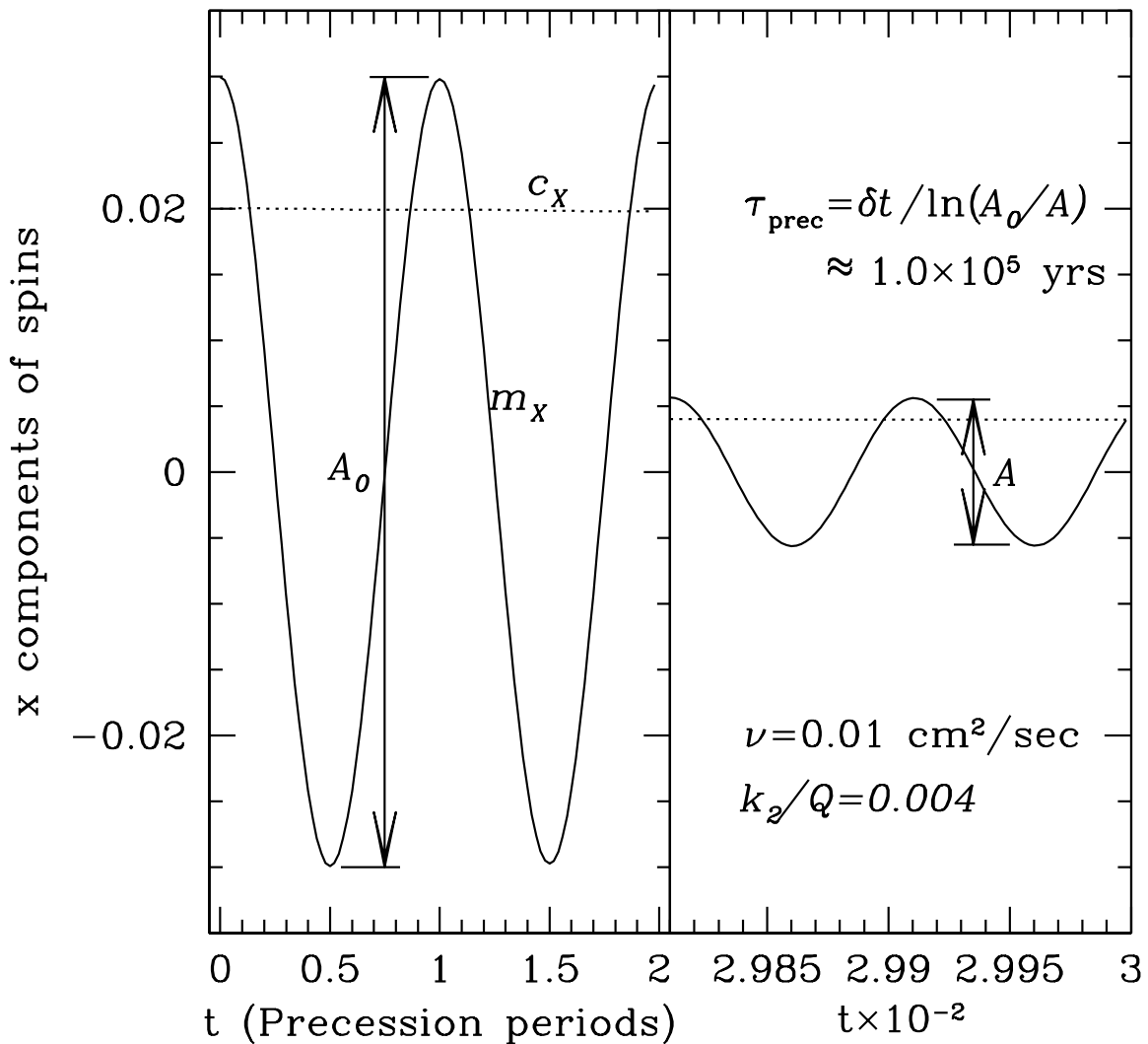


Fig. 3.— Numerically determined damping of Mercury’s free precession with core kinematic viscosity $\nu = 0.01 \text{ cm}^2/\text{sec}$ and tidal factor $k_2/Q_0 = 0.004$. m_x and c_x label the curves for the X components of the unit vectors along the mantle and core spin axes respectively. A_0 is a small but otherwise arbitrary initial amplitude.

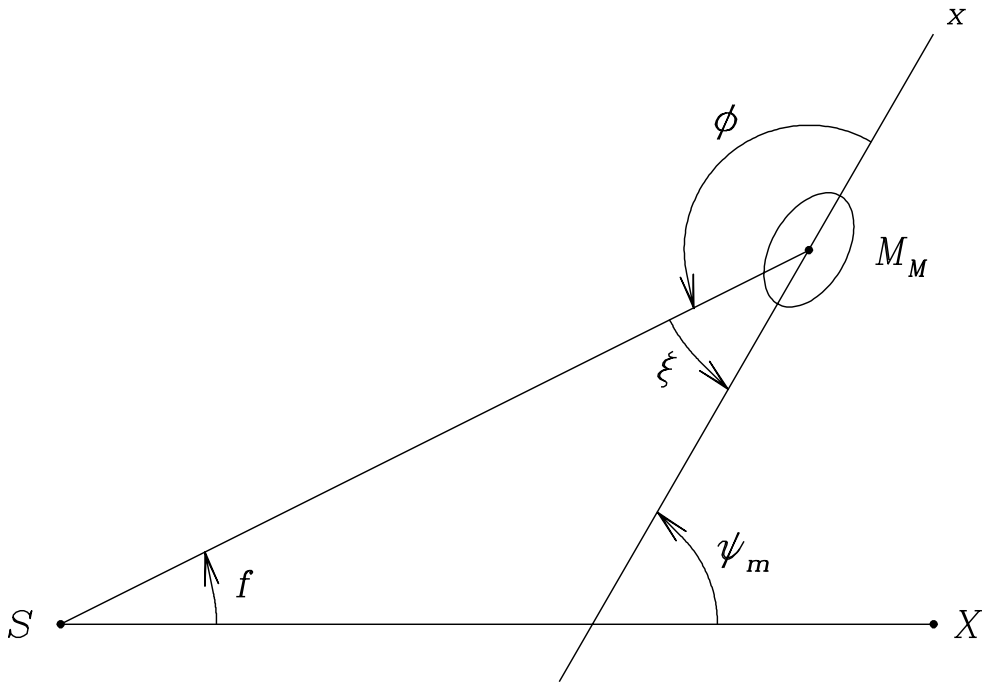


Fig. 4.— Angles used in the discussion of libration in longitude. SX is directed from the Sun to the perihelion of Mercury's orbit and M_M denotes Mercury, where x is the axis of minimum moment of inertia.

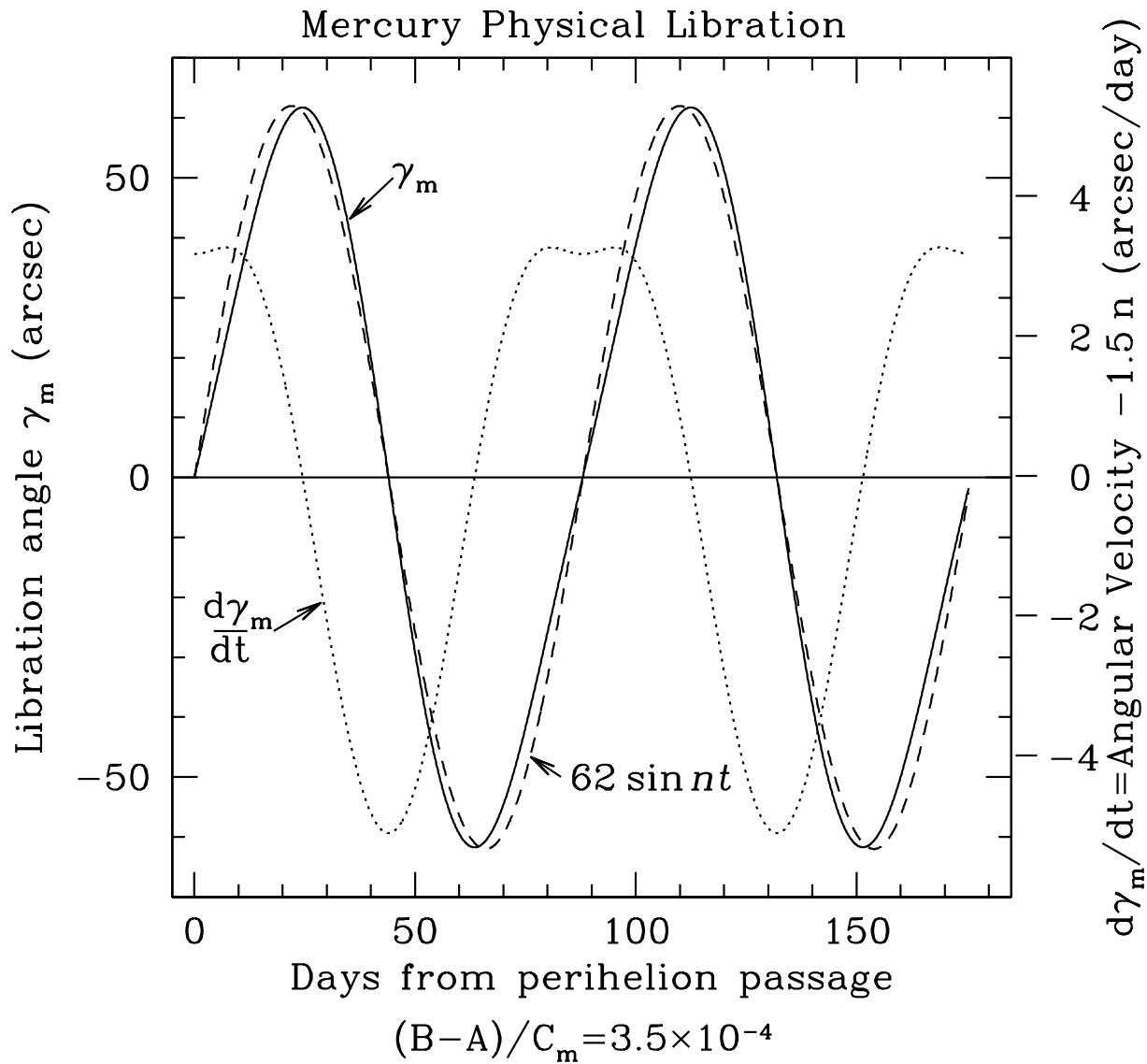


Fig. 5.— Forced libration of Mercury showing the deviations of the motions from pure harmonic form. The flat portion of $d\gamma_m/dt$ results from the fact that the rotation is nearly synchronous with the orbital motion for a range of true anomaly f on either side of the perihelion while the axis of minimum moment of inertia is nearly pointing to the Sun. (See Appendix B.)

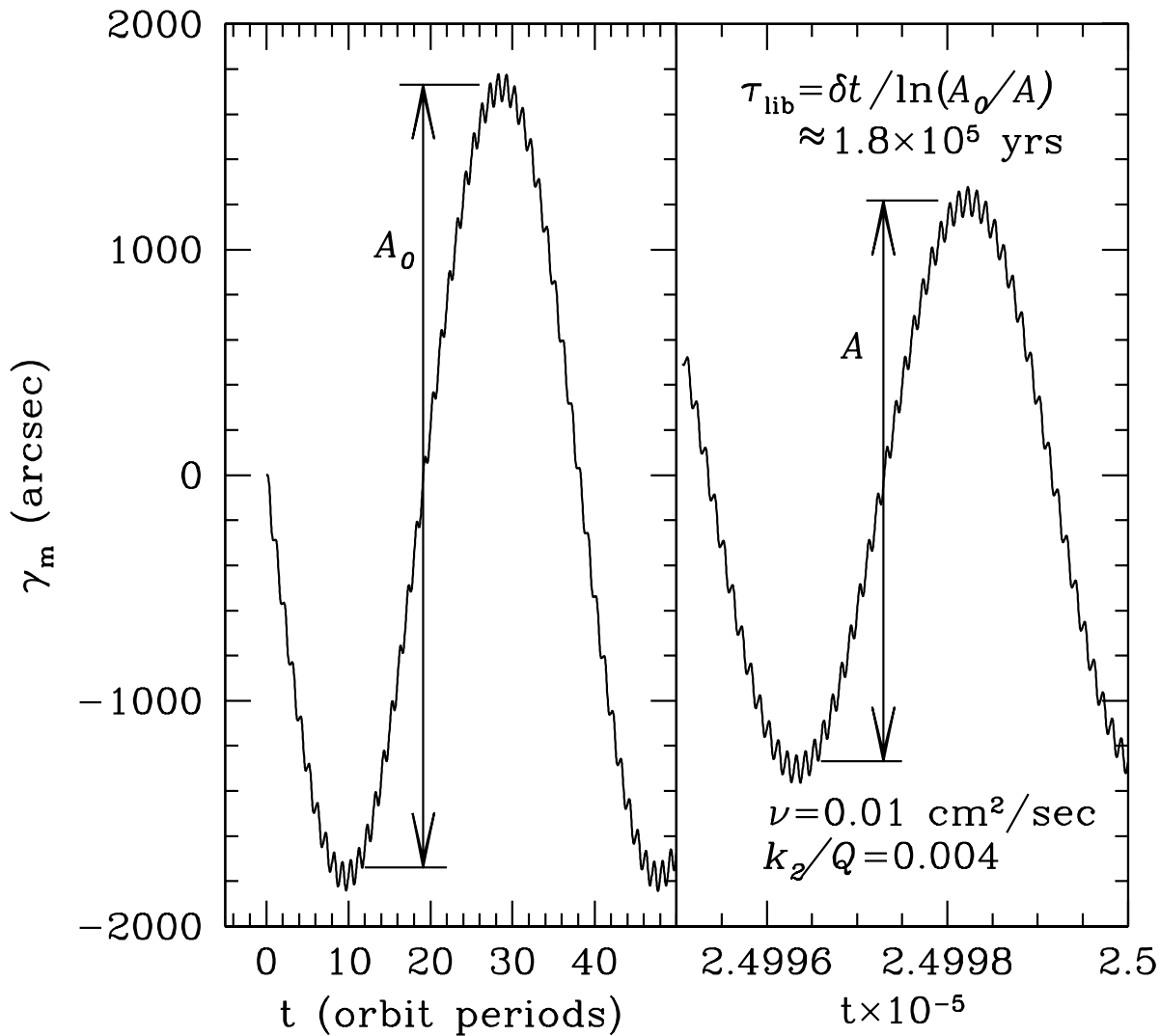


Fig. 6.— Numerically determined damping of Mercury’s free libration in longitude with core kinematic viscosity $\nu = 0.01 \text{ cm}^2/\text{sec}$ and tidal factor $k_2/Q_0 = 0.004$. The high frequency oscillations superposed on the free libration are the 88 day forced librations. $(B - A)/C_m = 3.5 \times 10^{-4}$ determines the free libration period of 9.2 years. A_0 is a small but otherwise arbitrary initial amplitude.